Superdiffusion and Lévy Flights

A Particle Transport Monte Carlo Simulation Code

Eduardo J. Nunes-Pereira

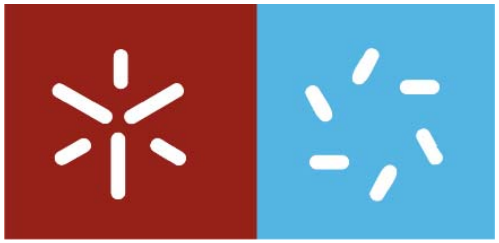

Centro de Física
Escola de Ciências
Universidade do Minho

ANOMALOUS TRANSPORT
Definitions and Examples

SUPERDIFFUSION AND LÉVY FLIGHTS
Serial code and opportunities for parallelization

DYNAMICS OF SUPERDIFFUSION
Numerical algorithms

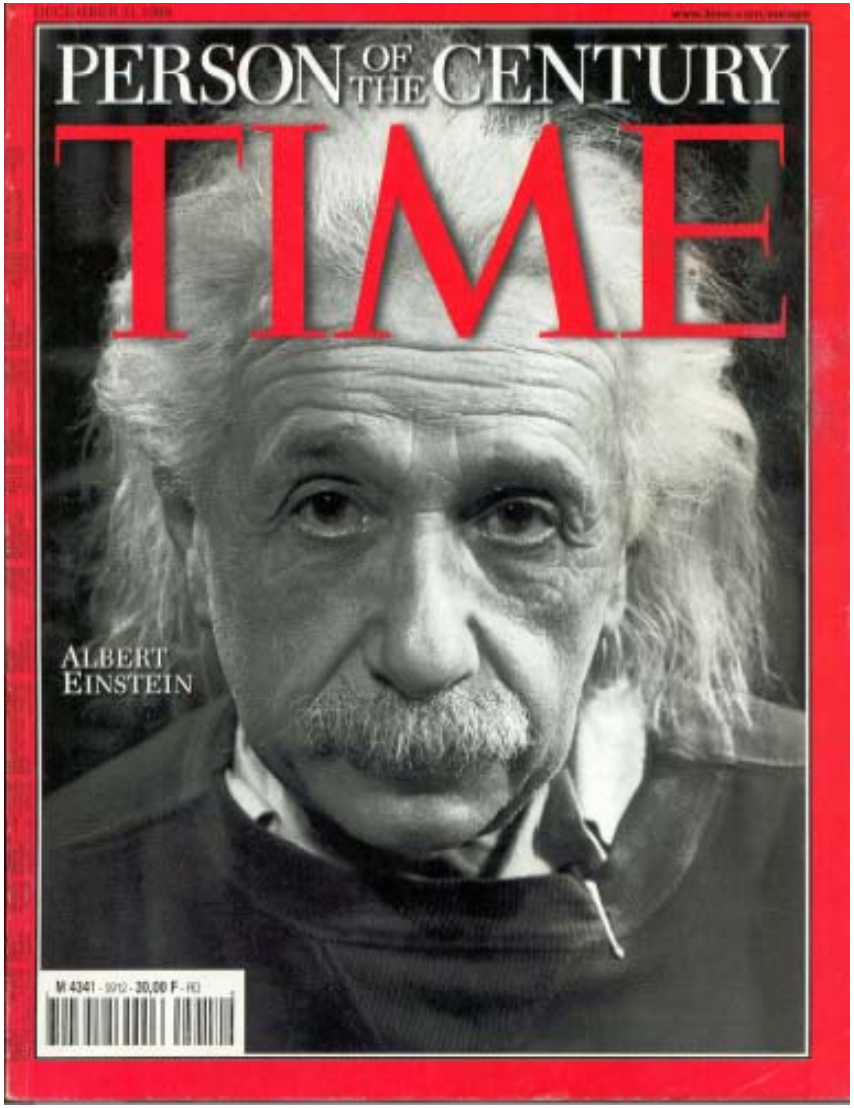
PERSON OF THE CENTURY
TIME
ALBERT
EINSTEIN

BROWNIAN MOTION
ONE OF PARADIGMS OF XX CENTURY

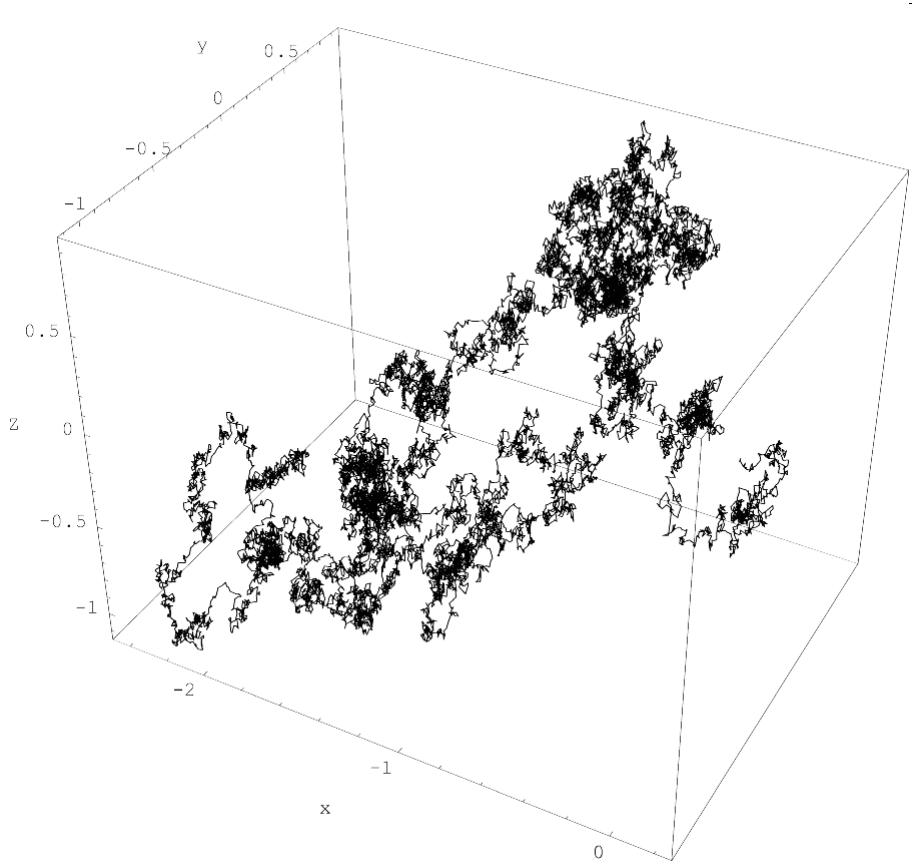

A single realisation of three-dimensional Brownian motion for times $0 \leq t \leq 2$

BROWNIAN MOTION
DIFFUSION EQUATION

$$\frac{\partial \rho}{\partial t} = D\frac{\partial^2 \rho}{\partial x^2}$$

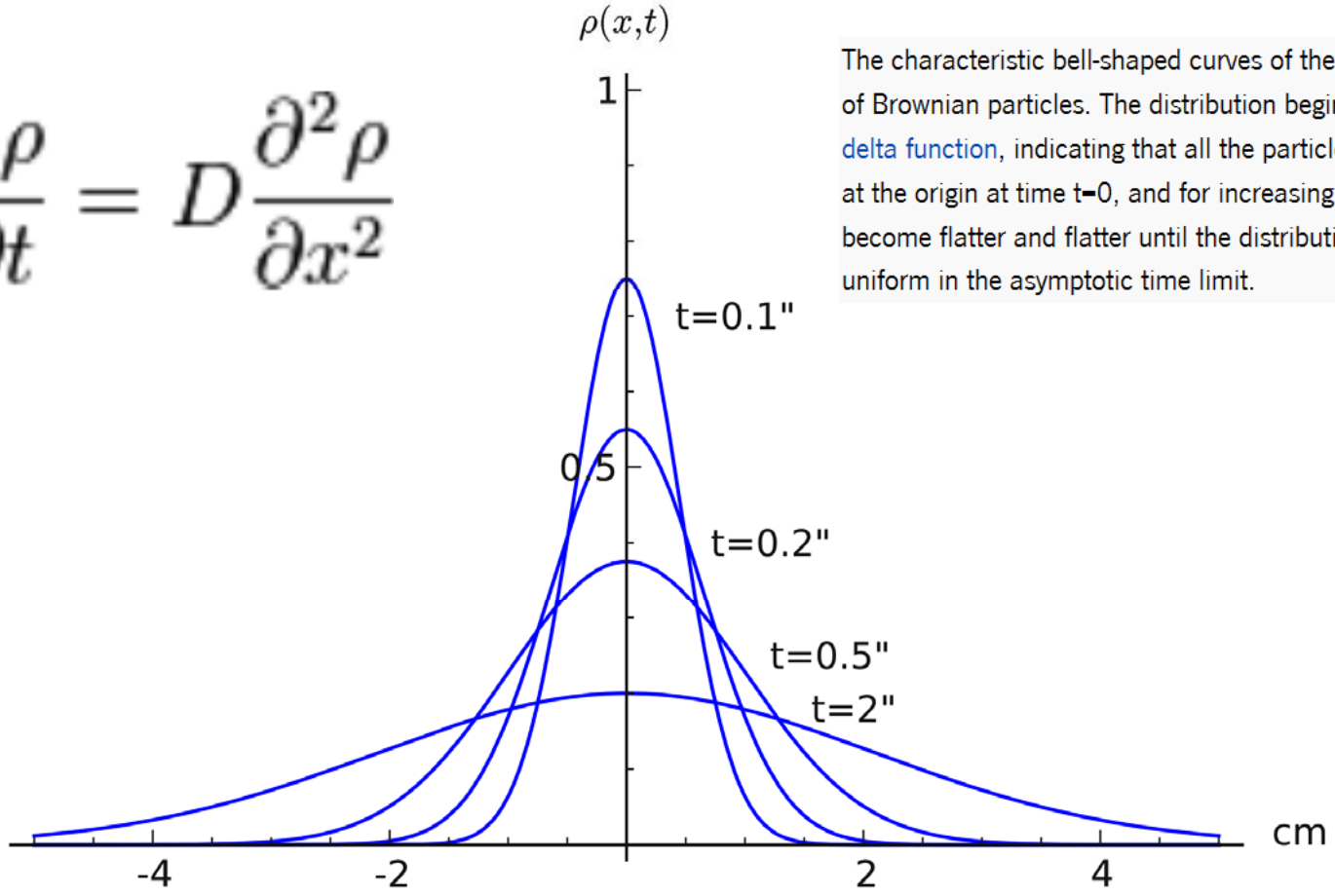

The characteristic bell-shaped curves of the diffusion of Brownian particles. The distribution begins as a Dirac delta function, indicating that all the particles are located at the origin at time t=0, and for increasing times they become flatter and flatter until the distribution becomes uniform in the asymptotic time limit.

$$\rho(x,t) = \frac{1}{(4\pi Dt)^{1/2}} e^{-x^2/4Dt} \qquad \overline{\Delta x^2} = 2Dt$$

ANOMALOUS TRANSPORT
WHY "ANOMALOUS" ? NOT VALID DIFFUSION EQ.

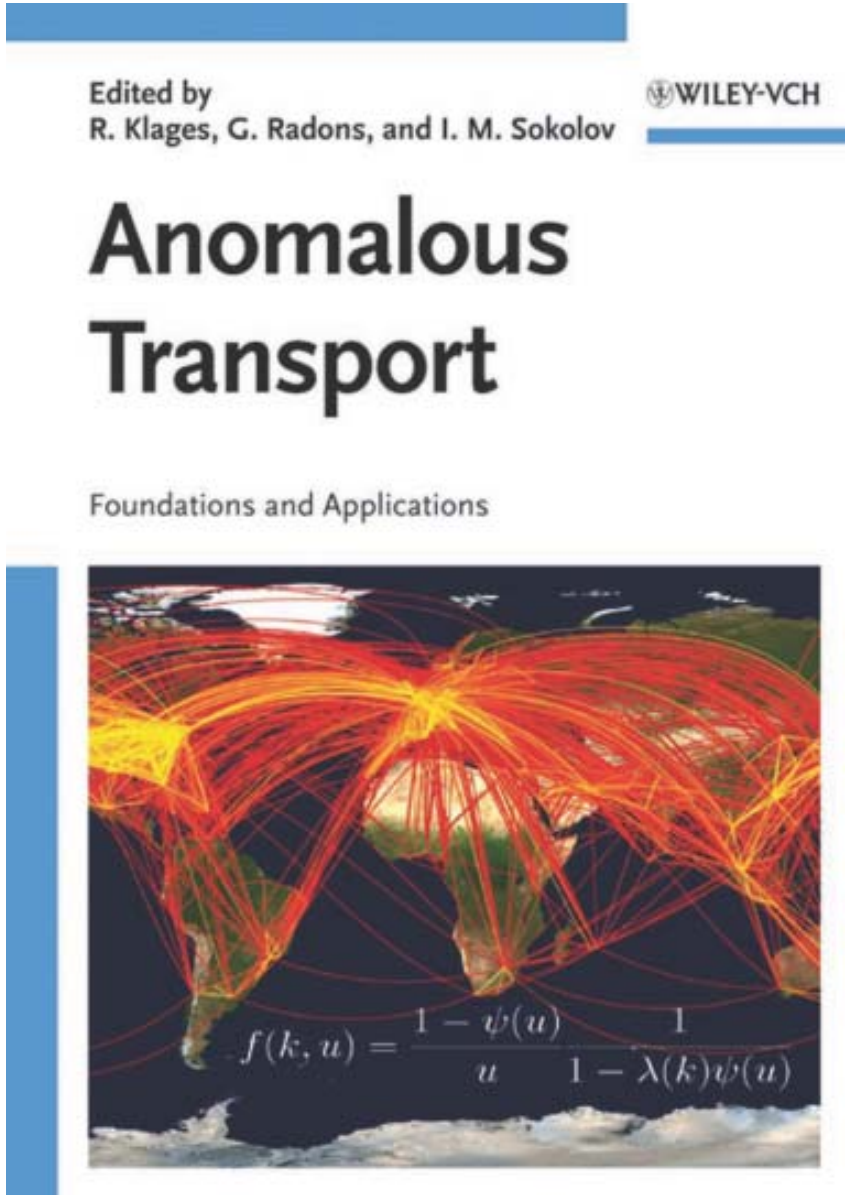

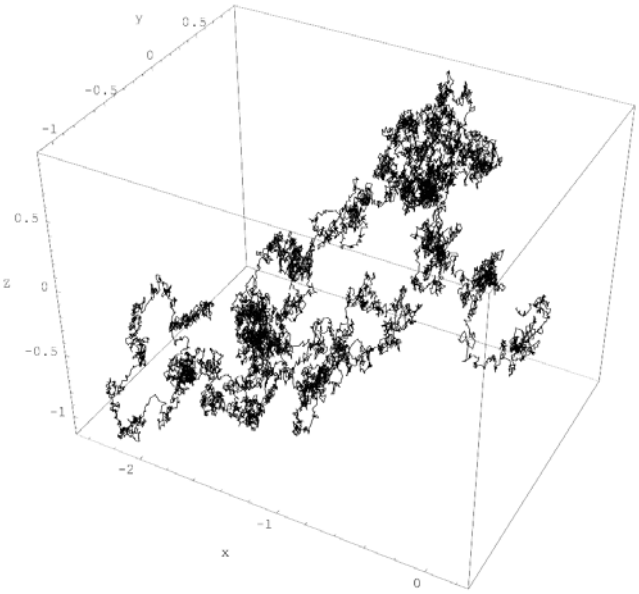

A single realisation of three-dimensional Brownian motion for times $0 \leq t \leq 2$

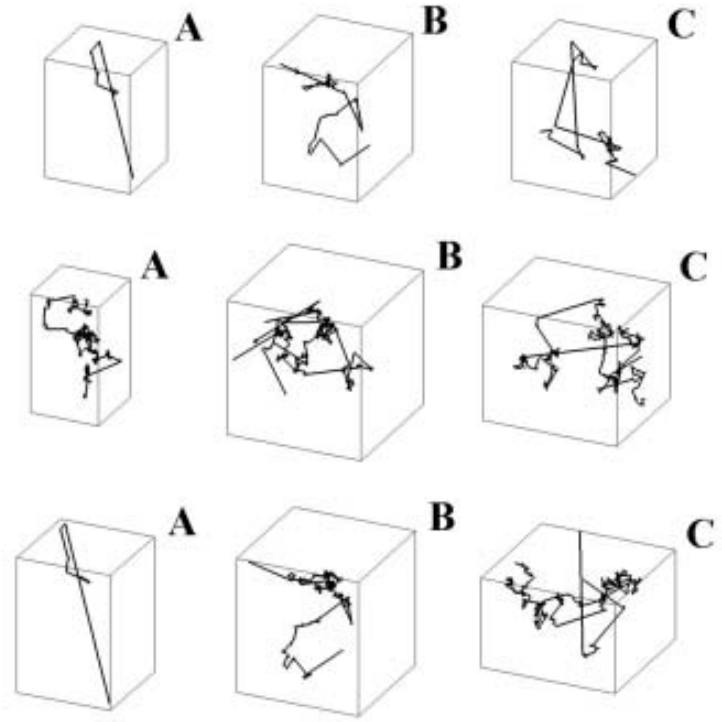

FIG. 3. Single trajectories of 50 000 jumps each for incoherent isotropic CFR radiation migration with Lorentz (top row), Doppler (middle row), and $a = 0.001$ Voigt (bottom row) profiles in infinite 3D medium. (A) shows the whole trajectory while (B) and (C) show successive details. The three trajectories were obtained with the same random number sequence.

Brownian motion
Characteristic scale
Mean Free Path
Diffusion Equation
Diffusion Coefficient

Anomalous Transport
No characteristic scale (fractal self-similar)
No second moment (sometimes no mean free path)
Diffusion Equation not valid
No Diffusion Coefficient

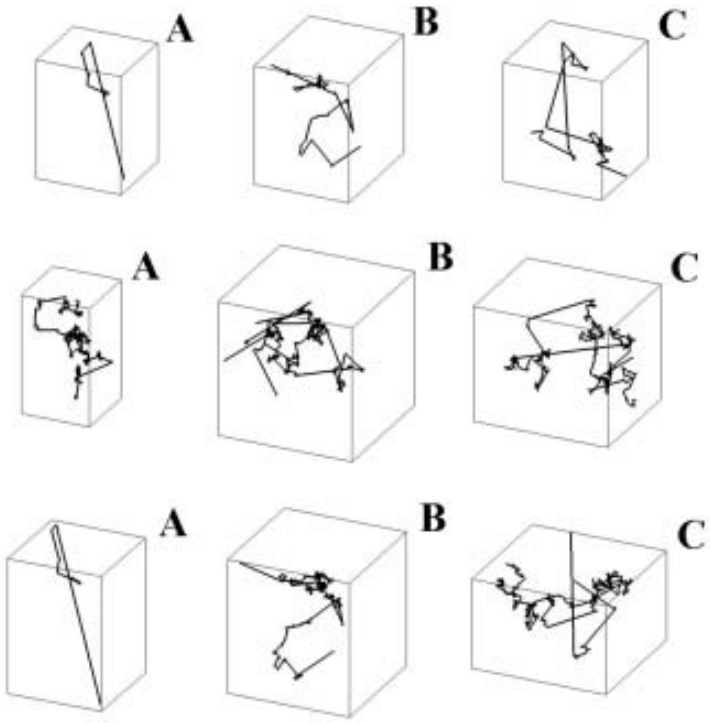

FIG. 3. Single trajectories of 50 000 jumps each for incoherent isotropic CFR radiation migration with Lorentz (top row), Doppler (middle row), and $a = 0.001$ Voigt (bottom row) profiles in infinite 3D medium. (A) shows the whole trajectory while (B) and (C) show successive details. The three trajectories were obtained with the same random number sequence.

Anomalous Transport
No characteristic scale

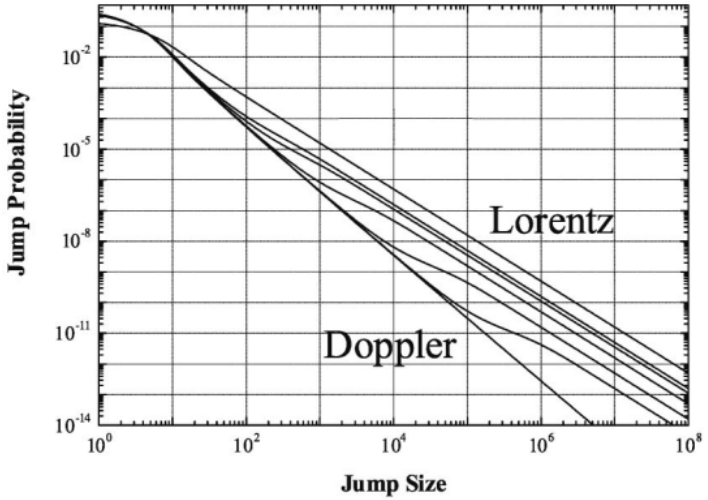

FIG. 1. Jump size distribution for CFR Doppler, Lorentz, and Voigt spectral profiles. From bottom to top: Doppler, Voigt with $a = 10^{-4}$, 10^{-3}, 0.01, 0.05, 0.1, and Lorentz.

Jump size distribution
Is a power law
(all scales; self similar fractal)

ANOMALOUS TRANSPORT (SUPERDIFFUSION)
PATHLENGTH DISTRIBUTION IS A POWER LAW
LÉVY FLIGHT
FLUORESCENT LAMPS

Photon Trajectories in Incoherent Atomic Radiation Trapping as Lévy Flights

Eduardo Pereira*
Universidade do Minho, Escola de Ciências, Departamento de Física, 4710-057 Braga, Portugal

José M. G. Martinho and Mário N. Berberan-Santos
Centro de Química-Física Molecular, Instituto Superior Técnico, 1049-001 Lisboa, Portugal
(Received 19 November 2003; published 13 September 2004)

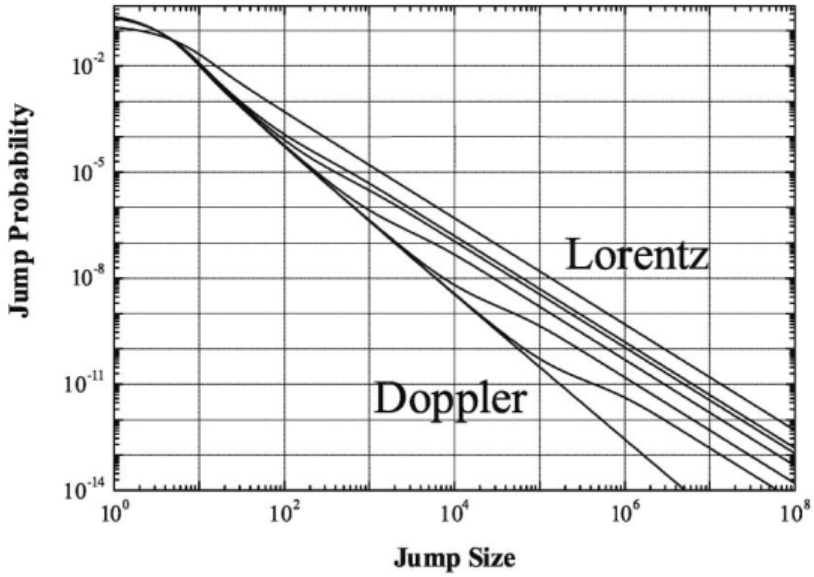

FIG. 1. Jump size distribution for CFR Doppler, Lorentz, and Voigt spectral profiles. From bottom to top: Doppler, Voigt with $a = 10^{-4}$, 10^{-3}, 0.01, 0.05, 0.1, and Lorentz.

ANOMALOUS TRANSPORT (SUPERDIFFUSION)
SUPERDIFUSION IS FASTER
(SUBDIFFUSION IS SLOWER; NOT SHOWN)

$$\langle x^2(t) \rangle \sim t^{\gamma}$$

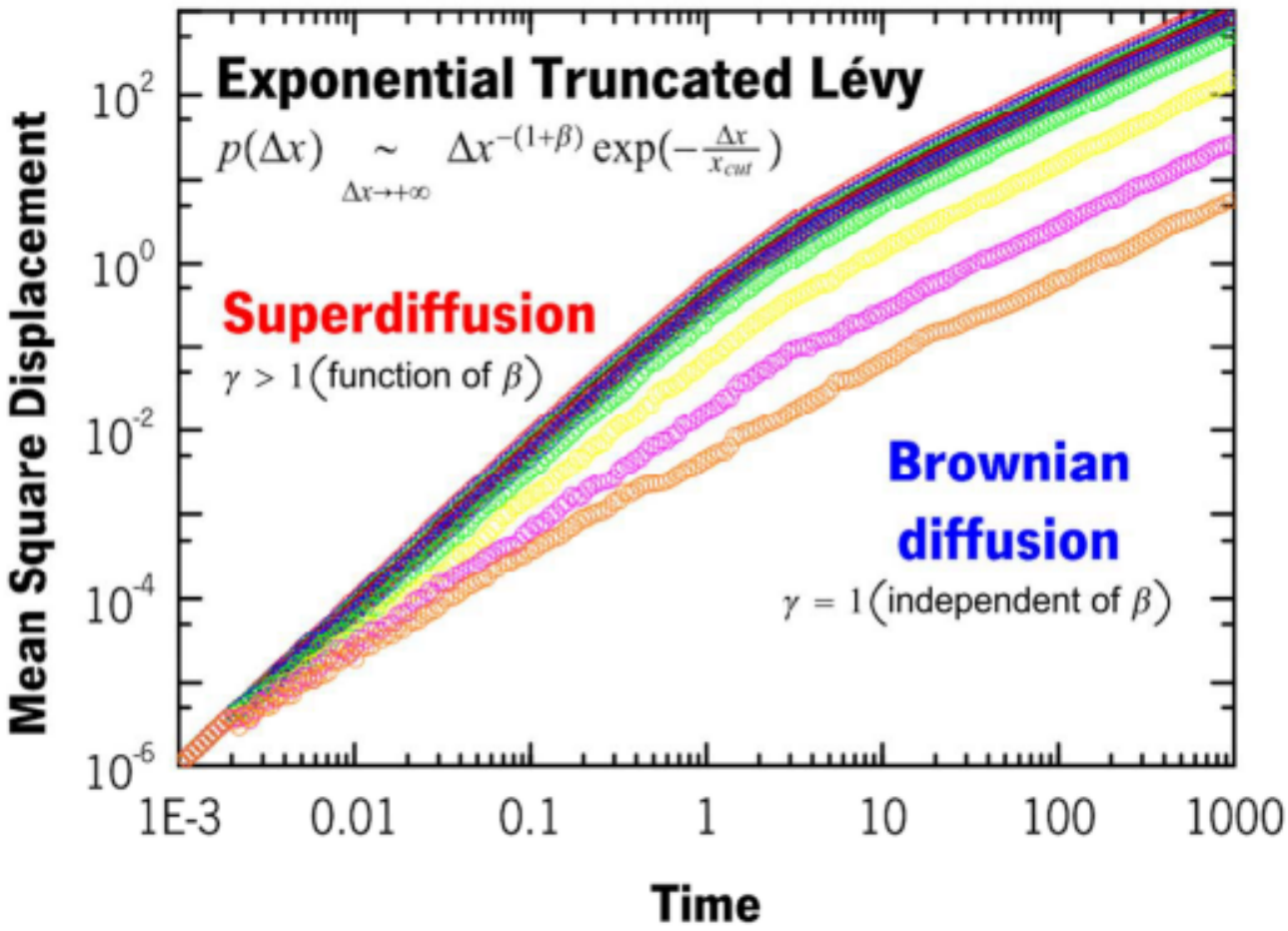

POWER LAWS (ARE EVERYWHERE)

Contemporary Physics, Vol. 46, No. 5, September–October 2005, 323–351

Taylor & Francis
Taylor & Francis Group

Power laws, Pareto distributions and Zipf's law

M.E.J. NEWMAN*

Department of Physics and Center for the Study of Complex Systems, University of Michigan, Ann Arbor, MI 48109, USA

(*Received 28 October 2004; in final form 23 November 2004*)

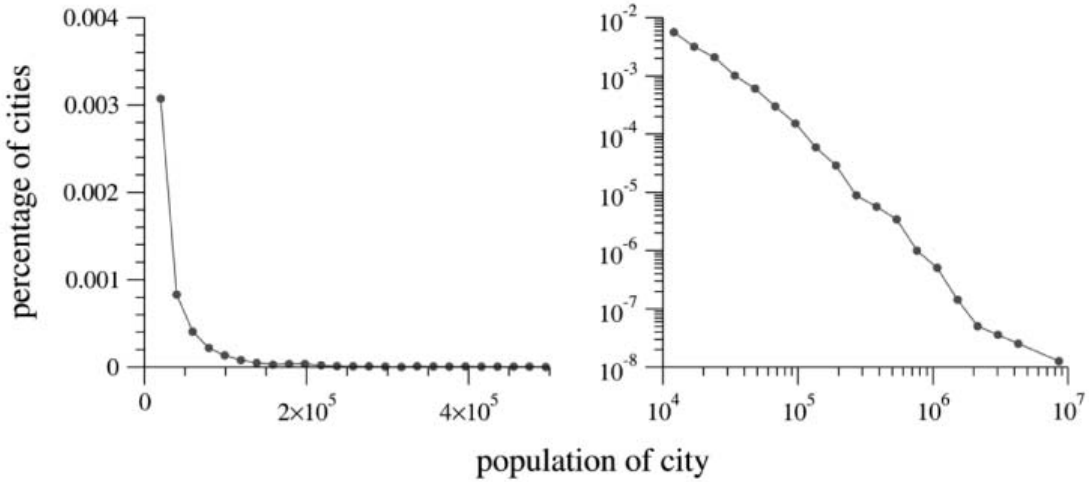

Figure 2. Left: histogram of the populations of all US cities with population of 10000 or more. Right: another histogram of the same data, but plotted on logarithmic scales. The approximate straight-line form of the histogram in the right panel implies that the distribution follows a power law. Data from the 2000 US Census.

POWER LAWS (ARE EVERYWHERE)

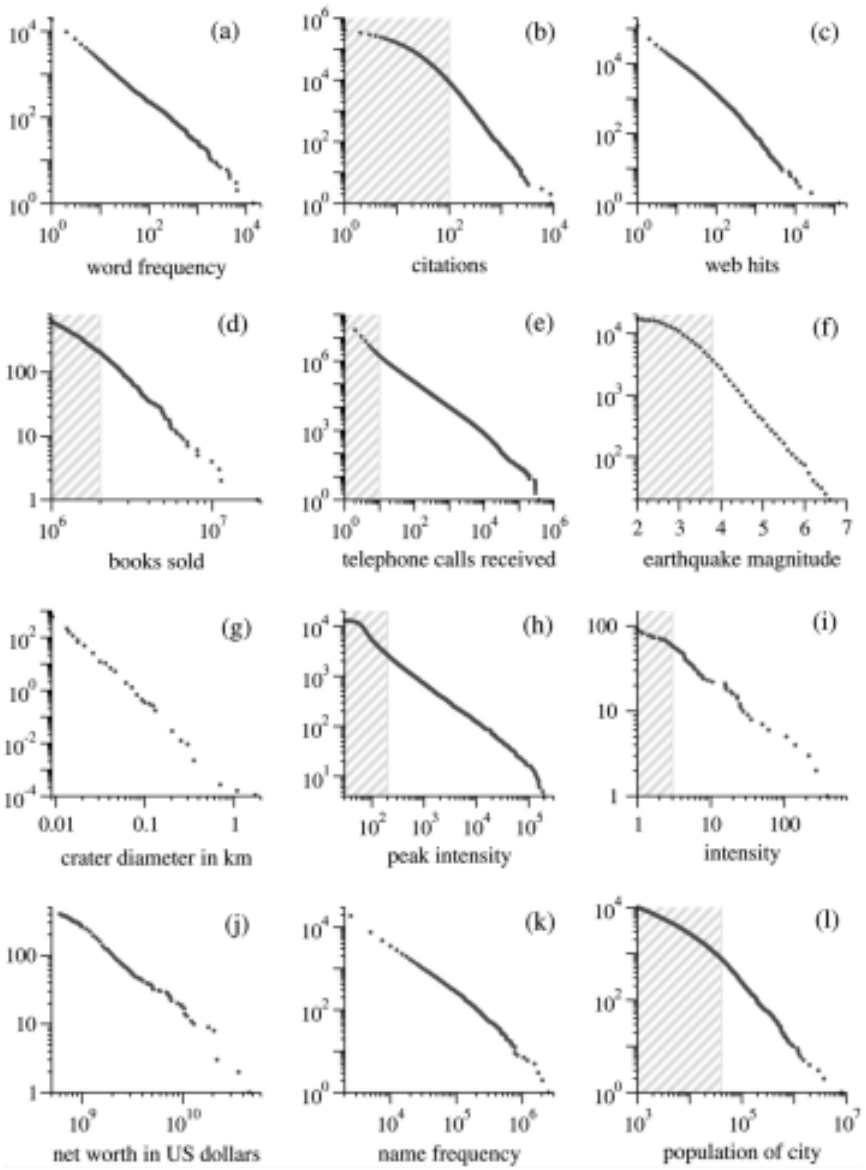

nature Vol 449|25 October 2007|doi:10.1038/nature06199

LETTERS

Revisiting Lévy flight search patterns of wandering albatrosses, bumblebees and deer

Andrew M. Edwards[1]†, Richard A. Phillips[1], Nicholas W. Watkins[1], Mervyn P. Freeman[1], Eugene J. Murphy[1], Vsevolod Afanasyev[1], Sergey V. Buldyrev[2,3], M. G. E. da Luz[4], E. P. Raposo[5], H. Eugene Stanley[2] & Gandhimohan M. Viswanathan[6]

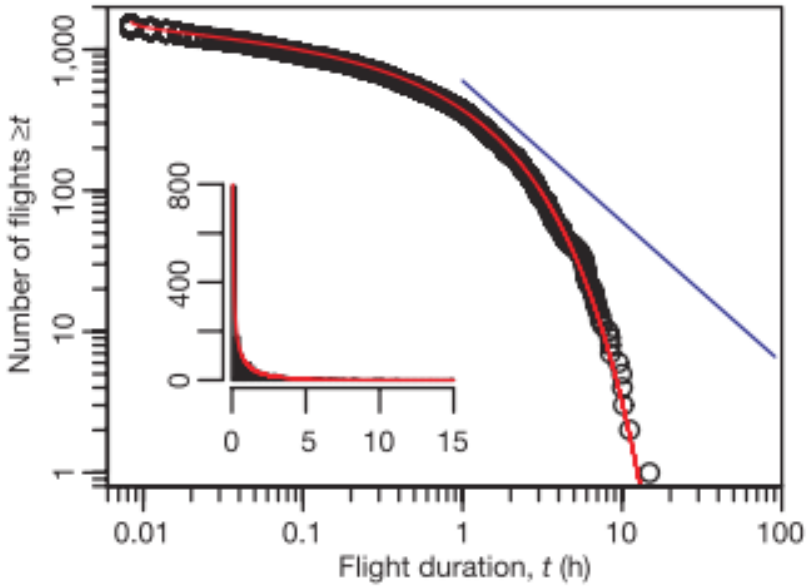

Figure 1 | Rank/frequency plot[23] of 2004 wandering albatross data, showing no evidence for Lévy flight behaviour. Circles show number of flights $\geq t$ for each flight duration t (calculated by ranking flights by size). The red curve is the fit to the shifted gamma distribution (equation (2)) with maximum likelihood estimates (MLEs) of $s = 0.31$ (95% confidence interval (CI): 0.27–0.34) and $r = 0.41\ \mathrm{h}^{-1}$ (95% CI: 0.36–0.46), obtained by maximizing the multinomial likelihood function that takes into account the discrete sampling nature of the loggers (see Supplementary Information). The data are consistent with coming from this distribution ($n = 1{,}416$, degrees of freedom = 37, $G = 28.9$, $P = 0.83$). Flights are correct to within ± 10 s (see Supplementary Information). If the flights ≥ 1 h followed the power law with exponent $\mu = 2$ as in ref. 7, the points would lie on the straight blue line[23] (that has been vertically shifted slightly for clarity)—this is clearly not the case. The inset shows the 2004 data as a conventional histogram on linear axes, with number of flights against flight duration in hours.

ANOMALOUS TRANSPORT – EXAMPLE 1
FORAGING BEHAVIOR IN SCARCE RESOURCES ENVIRONMENTS

nature Vol 451|28 February 2008|doi:10.1038/nature06518

LETTERS

Scaling laws of marine predator search behaviour

David W. Sims[1,2], Emily J. Southall[1], Nicolas E. Humphries[1], Graeme C. Hays[4], Corey J. A. Bradshaw[5]†, Jonathan W. Pitchford[6], Alex James[6,7], Mohammed Z. Ahmed[3], Andrew S. Brierley[8], Mark A. Hindell[9], David Morritt[10], Michael K. Musyl[11], David Righton[12], Emily L. C. Shepard[4], Victoria J. Wearmouth[1], Rory P. Wilson[4], Matthew J. Witt[13] & Julian D. Metcalfe[12]

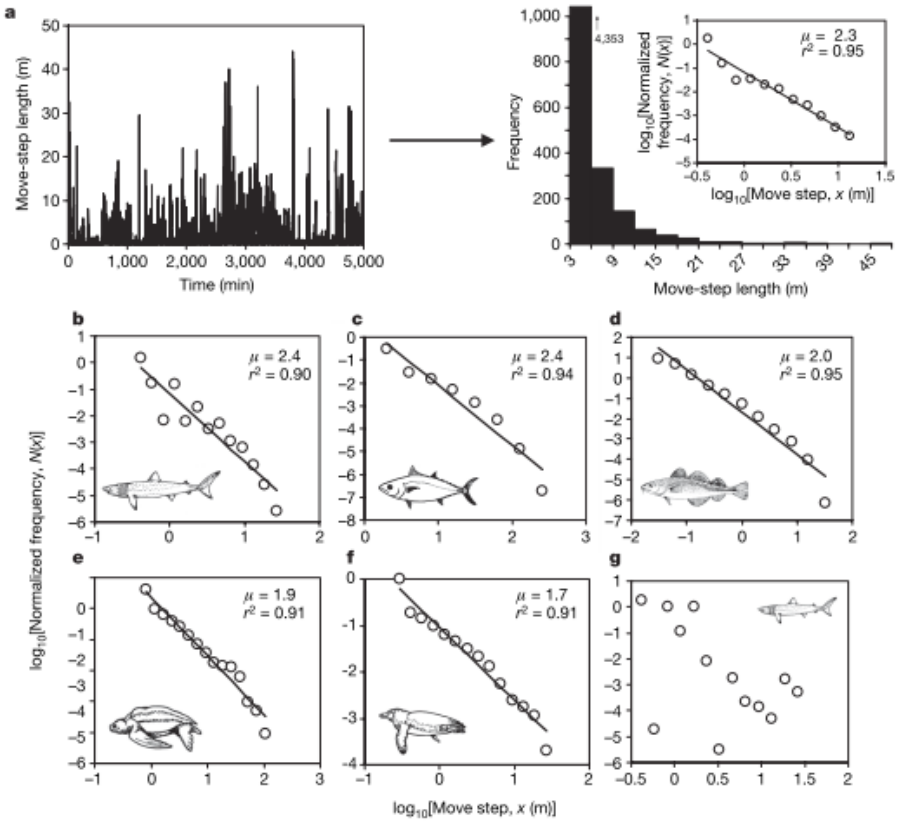

Figure 1 | Lévy-like scaling law among diverse marine vertebrates.

doi:10.1038/nature09116 nature

LETTERS

Environmental context explains Lévy and Brownian movement patterns of marine predators

Nicolas E. Humphries[1,2], Nuno Queiroz[1,3,4], Jennifer R. M. Dyer[1], Nicolas G. Pade[1,4], Michael K. Musyl[5], Kurt M. Schaefer[6], Daniel W. Fuller[6], Juerg M. Brunnschweiler[7], Thomas K. Doyle[8], Jonathan D. R. Houghton[9], Graeme C. Hays[10], Catherine S. Jones[4], Leslie R. Noble[4], Victoria J. Wearmouth[1], Emily J. Southall[1] & David W. Sims[1,2]

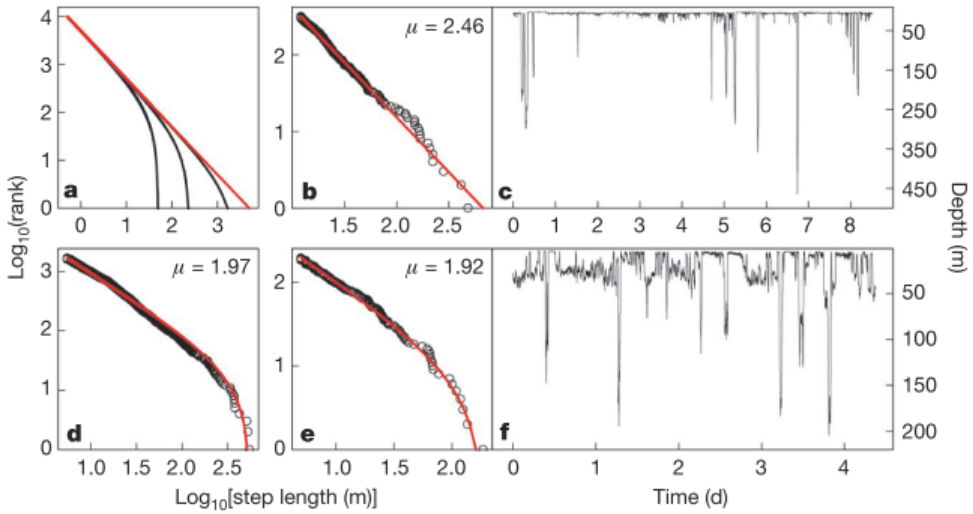

Figure 1 | Examples of good fits to power-law and truncated power-law distributions. **a**, Synthetic power-law and truncated power-law (Pareto) distributions with upper truncations set to 50, 250, 5,000. **b**–**f**, Empirical power-law and truncated power-law fits to dive data from individual blue sharks (*Prionace glauca*; **b**, **d**) and an ocean sunfish (*Mola mola*, **e**), together with the diving time series for the individual in **b** (over ~8 d; **c**) and the individual in **e** (over ~4 d; **f**). The red line indicates a synthetic power law in **a**, a power law in **b** and truncated power-law MLE model fits to empirical data in **d** and **e**.

ANOMALOUS TRANSPORT – EXAMPLE 1
ANIMAL TRACKING

ANOMALOUS TRANSPORT – EXAMPLE 2
POPULATION DYNAMICS AND EPIDEMICS

nature Vol 439|26 January 2006|doi:10.1038/nature04292

LETTERS

The scaling laws of human travel

D. Brockmann[1,2], L. Hufnagel[3] & T. Geisel[1,2,4]

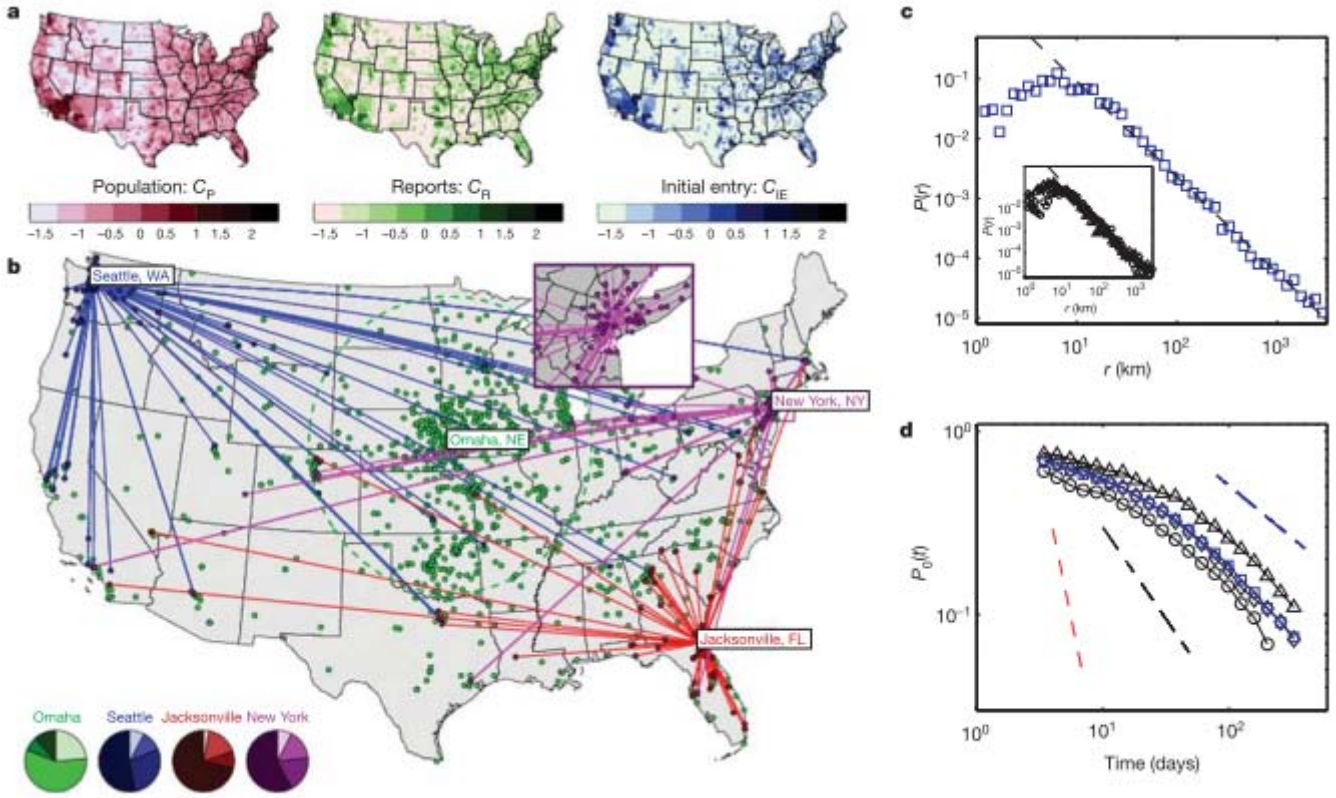

Figure 1 | Dispersal of bank notes and humans on geographical scales.

Vol 453|5 June 2008|doi:10.1038/nature06958 nature

LETTERS

Understanding individual human mobility patterns

Marta C. González[1], César A. Hidalgo[1,2] & Albert-László Barabási[1,2,3]

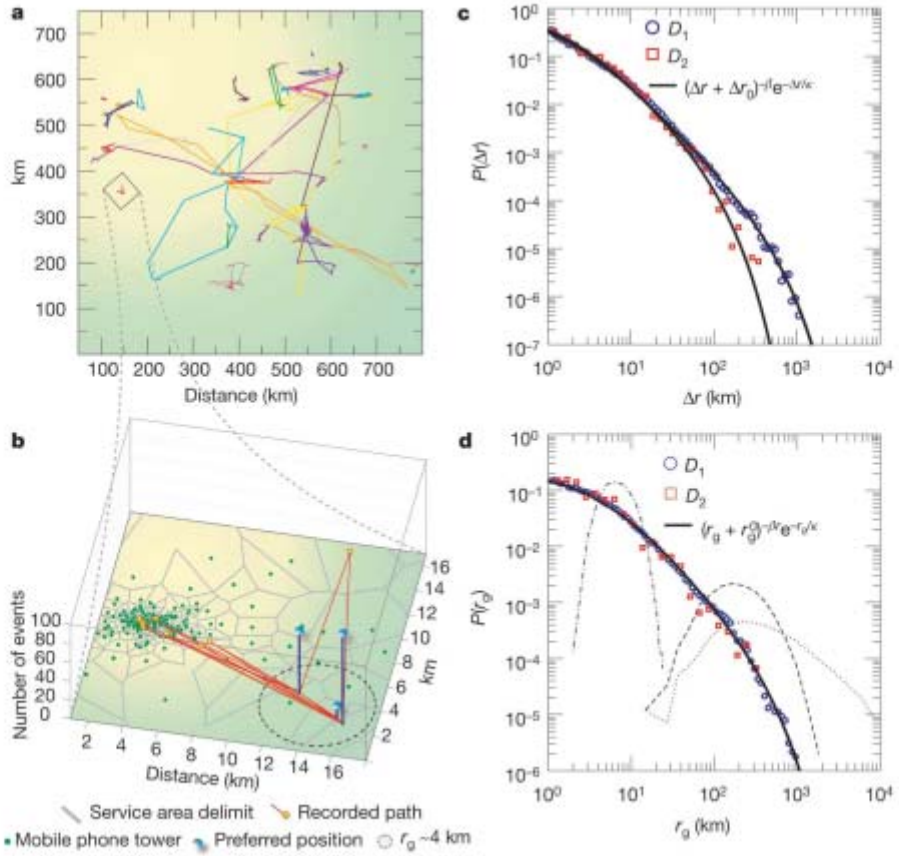

Figure 1 | Basic human mobility patterns.

ANOMALOUS TRANSPORT – EXAMPLE 2
POPULATION DYNAMICS AND EPIDEMICS

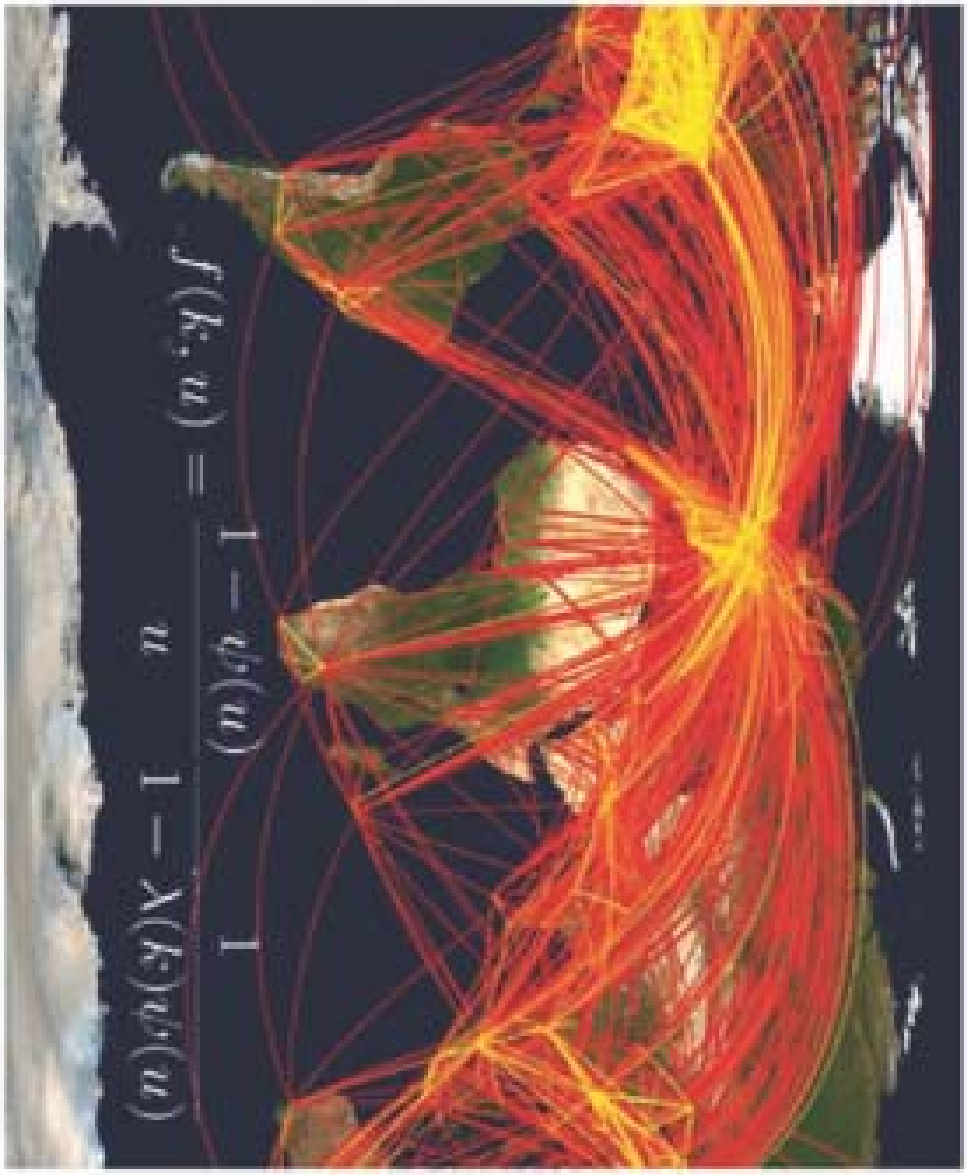

Power laws are helping researchers assess the risks posed by extreme natural hazards, while statistical physics may reveal an underlying universality in nature

Tails of natural hazards

Bruce D Malamud

4 Examples of power-law distributions

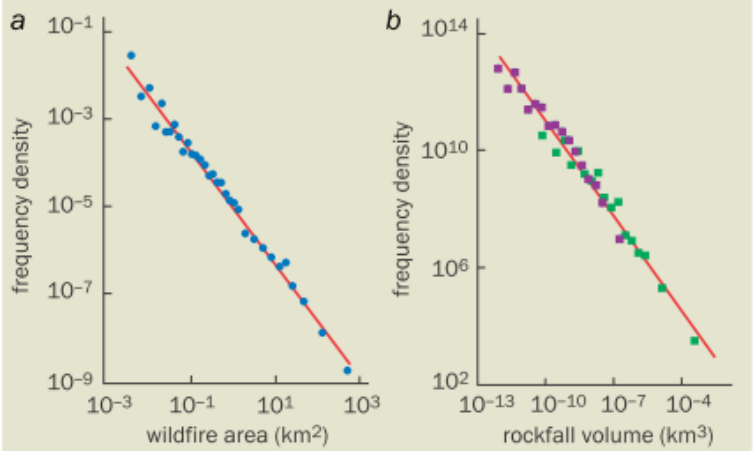

Power laws have been found to describe the frequency–size distributions of many natural hazards. (*a*) Wildfires in the Mediterranean eco-region of the US. Frequency densities, *f*, (i.e. the number of fires per unit area "bin" per year per eco-region area) are plotted as a function of the area of the wildfire, A_F. Fitting the data with a power law gives excellent agreement with $f = 1.0 \times 10^{-5} A_F^{-1.3}$ (i.e. a straight line on logarithmic axes) for wildfire areas between about 0.01 to 1000 km^2. (*b*) Rockfalls also follow such power-law behaviour. Here the number of rockfalls per unit volume bin is plotted as a function of their volume, V_R, for two different datasets: an earthquake-triggered rockslide event in Umbria, Italy, in 1997 (purple) and historical data from Yosemite between 1980 and 2002 (green). Despite taking place under very different conditions, the datasets follow a power law of the form $2.34 V_R^{-1.07}$ remarkably well for rock volumes between 0.001 to 1000 000 m^3.

ANOMALOUS TRANSPORT – EXAMPLE 4
ANOMALOUS TRASPORT FOR LIGHT
SUPERDIFFUSIVE RADIATIVE TRANSPORT

Vol 453|22 May 2008|doi:10.1038/nature06948 nature

LETTERS

A Lévy flight for light

Pierre Barthelemy[1], Jacopo Bertolotti[1] & Diederik S. Wiersma[1]

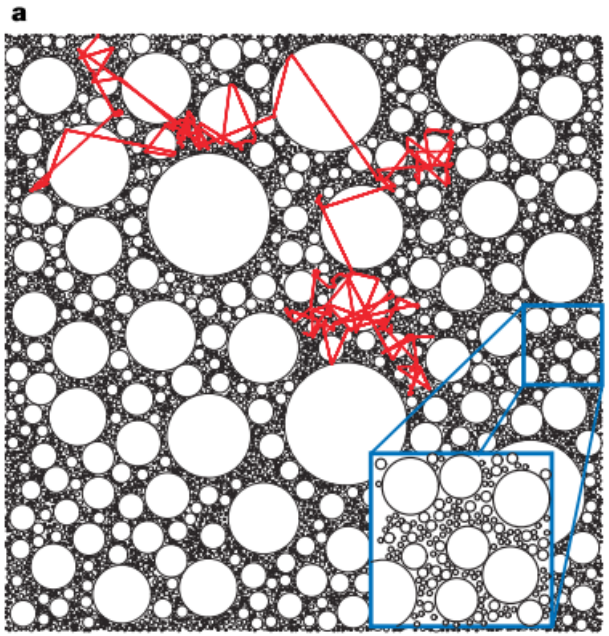

Figure 5 | Lévy walk in an inhomogeneous medium. a, Random walker trajectory, obtained by Monte Carlo simulation. Owing to the strong density fluctuations, the scattering material permits Lévy flights (red). Inset, magnification showing the scale invariance of the material's structure.

ANOMALOUS TRANSPORT – EXAMPLE 4
ANOMALOUS TRASPORT FOR LIGHT
SUPERDIFFUSIVE RADIATIVE TRANSPORT

Vol 453|22 May 2008|doi:10.1038/nature06948 nature

LETTERS

A Lévy flight for light

Pierre Barthelemy[1], Jacopo Bertolotti[1] & Diederik S. Wiersma[1]

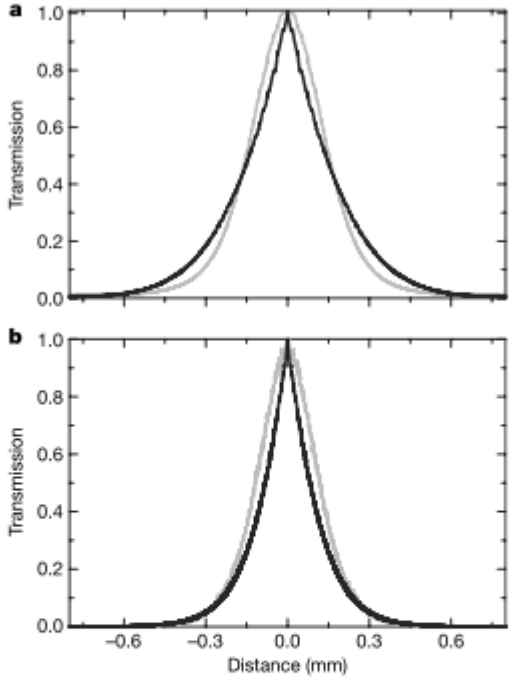

Figure 4 | Average transmission on the output surface versus radial distance from the centre. **a**, Experimental data. In the Lévy case (black) an average over 3,000 sample configurations was needed to obtain the average behaviour. The profile of the Lévy sample shows a pronounced cusp, and slowly decaying tails. The normal diffusive sample (grey) has a profile close to a gaussian lineshape: the top is rounded and long tails are absent. **b**, Result of Monte Carlo simulations of a normal diffusive random walk (grey) and a Lévy random walk (black) in a slab. The superdiffusive profile again displays a sharp cusp and decays more slowly than does the normal diffusive profile. The difference in absolute widths between experiment and simulation is due to internal reflections at the boundary of the sample, which were not taken in account in the simulations.

ANOMALOUS TRANSPORT
Definitions and Examples

SUPERDIFFUSION AND LÉVY FLIGHTS
Serial code and opportunities for parallelization

DYNAMICS OF SUPERDIFFUSION
Numerical algorithms

SUPERDIFFUSIVE RADIATIVE TRANSPORT

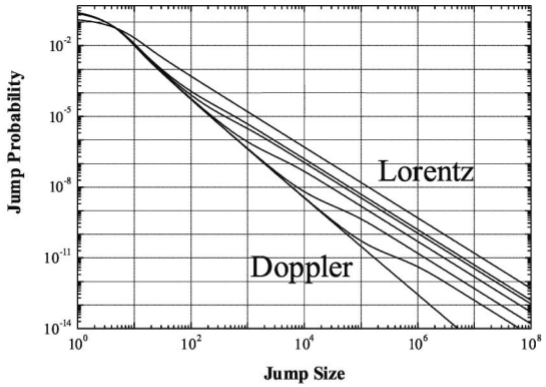

FIG. 1. Jump size distribution for CFR Doppler, Lorentz, and Voigt spectral profiles. From bottom to top: Doppler, Voigt with $a = 10^{-4}$, 10^{-3}, 0.01, 0.05, 0.1, and Lorentz.

THEORY

ARTICLES
PUBLISHED ONLINE: 31 MAY 2009 | DOI: 10.1038/NPHYS1286
nature physics

Lévy flights of photons in hot atomic vapours

N. Mercadier[1], W. Guerin[1], M. Chevrollier[2] and R. Kaiser[1]*

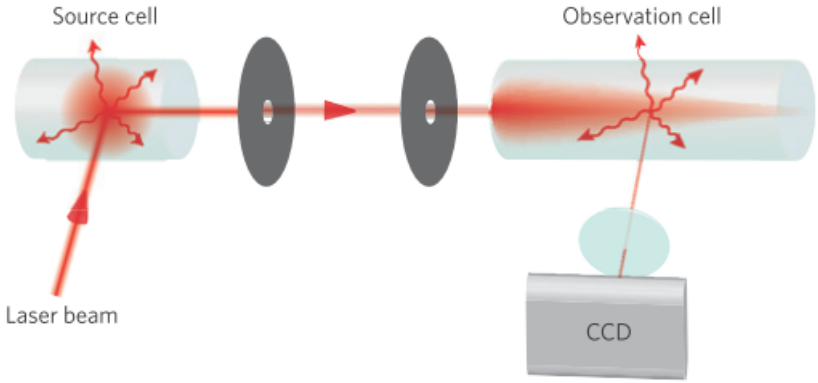

Figure 1 | The experimental set-up. A laser beam is incident on a so-called source cell filled with rubidium vapour. Scattered light propagating at an orthogonal direction is selected with two diaphragms and illuminates a second, observation cell. The light scattered in this second cell is imaged on a cooled CCD camera. This fluorescence signal is proportional to the step-size distribution function.

VERIFIED EXPERIMENTALLY

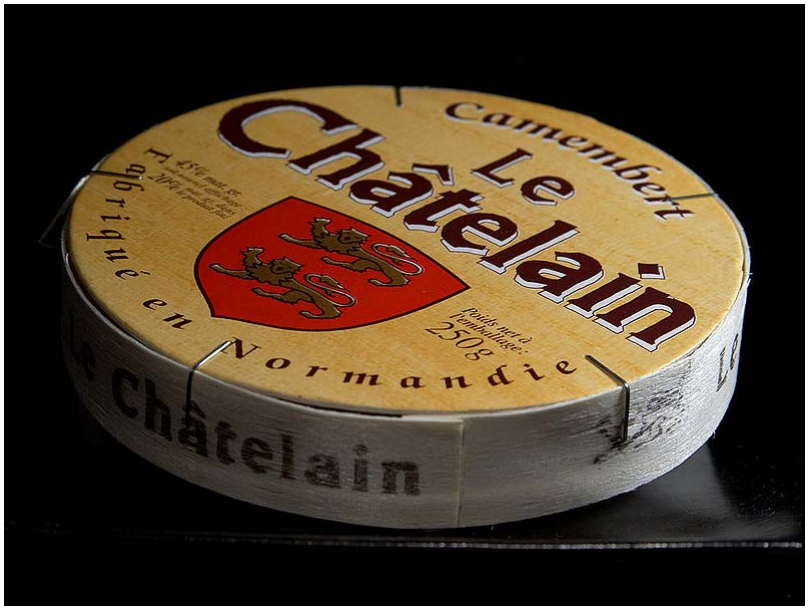

“LE CAMEMBERT” EXPERIMENT
(with R.KAISER, NICE)
Transmission profile under superdiffusion ...

A Lévy flight for light

Pierre Barthelemy[1], Jacopo Bertolotti[1] & Diederik S. Wiersma[1]

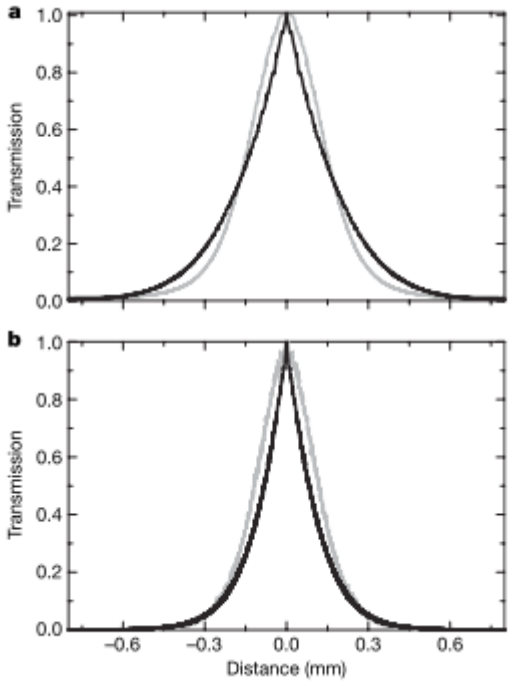

SUPERDIFFUSIVE RADIATIVE TRANSPORT
WITH POWER LAWS (LÉVY FLIGHTS)
PARTICLE (LIGHT) TRANSPORT MONTE CARLO SIMULATION

SUPERDIFFUSIVE RADIATIVE TRANSPORT
WITH POWER LAWS (LÉVY FLIGHTS)
PARTICLE (LIGHT) TRANSPORT MONTE CARLO SIMULATION

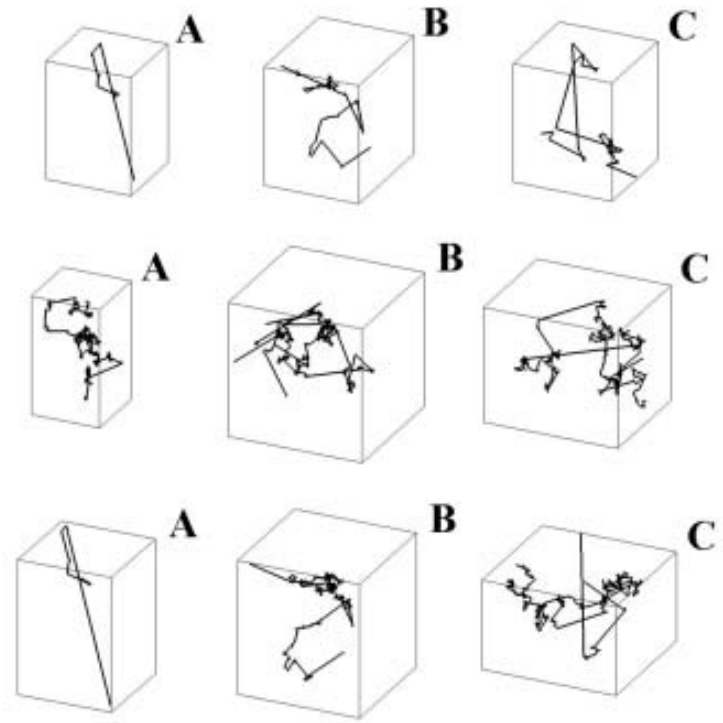

FIG. 3. Single trajectories of 50 000 jumps each for incoherent isotropic CFR radiation migration with Lorentz (top row), Doppler (middle row), and $a = 0.001$ Voigt (bottom row) profiles in infinite 3D medium. (A) shows the whole trajectory while (B) and (C) show successive details. The three trajectories were obtained with the same random number sequence.

PARTICLE (LIGHT) TRANSPORT
MONTE CARLO SIMULATION
GENERATE TRAJECTORIES AND
KEEP TRACK AND ACCUMULATE

MONTE CARLO
MASSIVE USE OF RANDOM NUMBERS
SLOW CONVERGENCE STATISTICS
(MONTE CARLO)
AND
POWER LAWS (EVENTS IN THE TAIL
OF THE DISTRIBUTION DOMINANT)

HIGH NUMBER OF TRAJECTORIES

SERIAL RANDOM NUMBER GENERATORS
PORTABLE, PSEUDO-RANDOM NUMBERS GENERATORS

STEP 1: UNIFORM DEVIATES IN [0,1[

$$p(x)dx = \begin{cases} dx & 0 \le x < 1 \\ 0 & \text{otherwise} \end{cases}$$

$x \sim \mathrm{U}(0,1)$ **x is distributed uniformly in [0,1[**

STEP 2 (EXAMPLE): EXPONENTIAL DEVIATES

$$p(y)dy$$

$$|p(y)dy| = |p(x)dx|$$

$$p(y) = p(x)\left|\frac{dx}{dy}\right|$$

$$y(x) = -\ln(x) \qquad x \sim \mathrm{U}(0,1)$$

$$p(y)dy = \left|\frac{dx}{dy}\right| dy = e^{-y}dy$$

SERIAL RANDOM NUMBER GENERATORS
PORTABLE, PSEUDO-RANDOM NUMBERS GENERATORS

STEP 3: GENERAL TRANSFORMATION METHOD (FOR ANY STATISTICAL DISTRIBUTION)

Solve ... $\frac{dx}{dy} = f(y)$ with $x \sim \mathrm{U}(0,1)$

$$x = F(y)$$

$$F(y) = \int_0^y p(y)\,dy$$

Indefinite integral of desired distribution

$$\boxed{y(x) = F^{-1}(x)}$$

SOLVE ANALYTICALLY OR NUMERICALLY

STEP 2 (EXAMPLE): EXPONENTIAL DEVIATES – ANALYTICAL

$$F(y) = \int_0^y p(y)\,dy = \int_0^y e^{-y}dy = 1 - e^{-y}$$

$$x = F(y)$$

$$y(x) = F^{-1}(x) = -ln(1-x) = -ln(x)$$

SERIAL RANDOM NUMBER GENERATORS
PORTABLE, PSEUDO-RANDOM NUMBERS GENERATORS

STEP 3: GENERAL TRANSFORMATION METHOD
(FOR ANY STATISTICAL DISTRIBUTION)

$$y(x) = F^{-1}(x)$$

SOLVE ANALYTICALLY OR NUMERICALLY

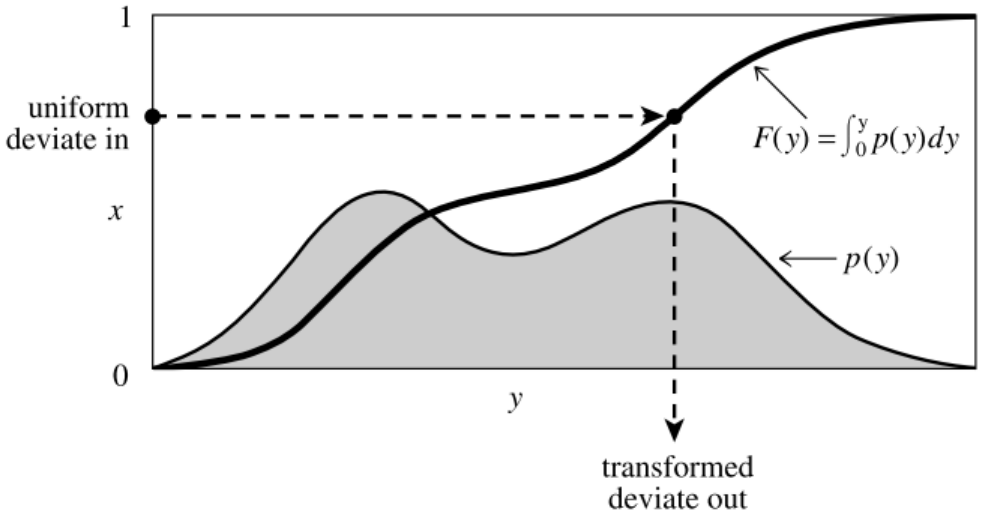

Figure 7.3.1. Transformation method for generating a random deviate y from a known probability distribution $p(y)$. The indefinite integral of $p(y)$ must be known and invertible. A uniform deviate x is chosen between 0 and 1. Its corresponding y on the definite-integral curve is the desired deviate.

RANDOM NUMBER GENERATORS
IN SERIAL CODE FOR SUPERDIFFUSIVE RADIATIVE TRANSPORT

STEP 1: UNIFORM DEVIATES IN [0,1[

$$p(x)dx = \begin{cases} dx & 0 \le x < 1 \\ 0 & \text{otherwise} \end{cases}$$

$x \sim \mathrm{U}(0,1)$ **x is distributed uniformly in [0,1[**

BASIC ALGORITHM – LINEAR CONGRENTIAL GENERATOR

$$I_{j+1} = aI_j + c \pmod{m}$$

INTEGER ARITHMETIC

$I_{j+1} \;/\; m$ **IS THE DESIRED REAL RANDOM NUMBER**

SEED + "SET OF MAGIC NUMBERS", FOR MAXIMUM REPETITION PERIOD

RANDOM NUMBER GENERATORS
IN SERIAL CODE FOR SUPERDIFFUSIVE RADIATIVE TRANSPORT

ran2 "NUMERICAL RECIPES"
2 GENERATORS PLUS ADDITIONAL SHUFFLING PROCEDURE
(BREAK SEQUENTIAL CORRELATION)

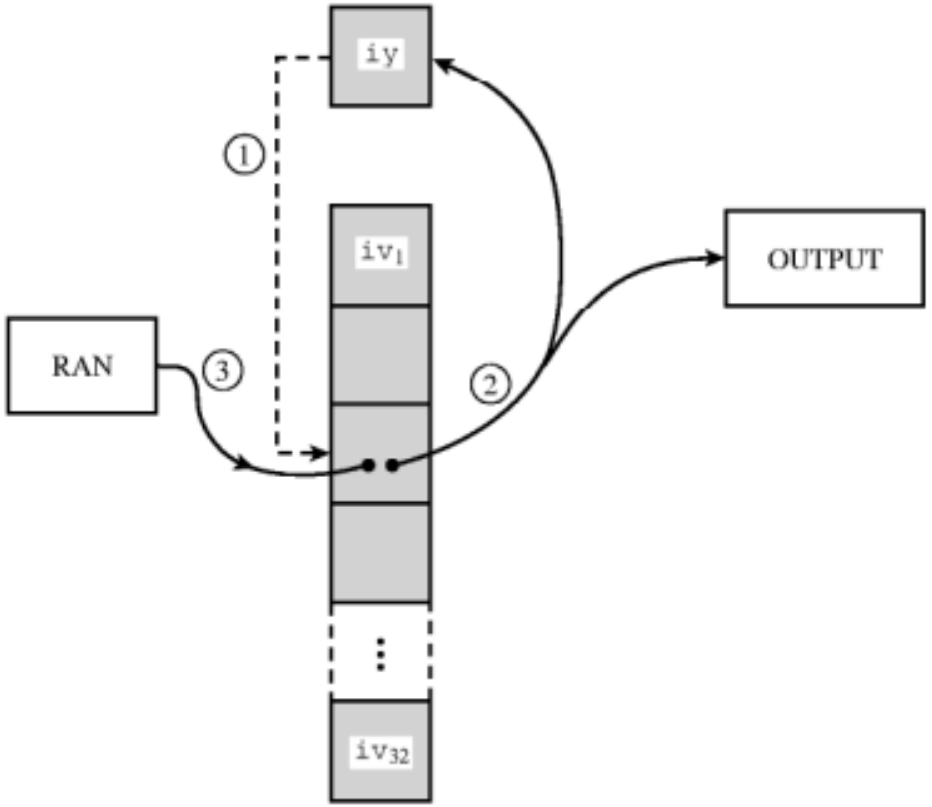

Figure 7.1.1. Shuffling procedure used in `ran1` to break up sequential correlations in the Minimal Standard generator. Circled numbers indicate the sequence of events: On each call, the random number in `iy` is used to choose a random element in the array `iv`. That element becomes the output random number, and also is the next `iy`. Its spot in `iv` is refilled from the Minimal Standard routine.

RANDOM NUMBER GENERATORS
IN SERIAL CODE FOR SUPERDIFFUSIVE RADIATIVE TRANSPORT

ANALYTICAL GENERAL TRANSFORMATION METHOD
IN MONTE CARLO TRAJECTORIES

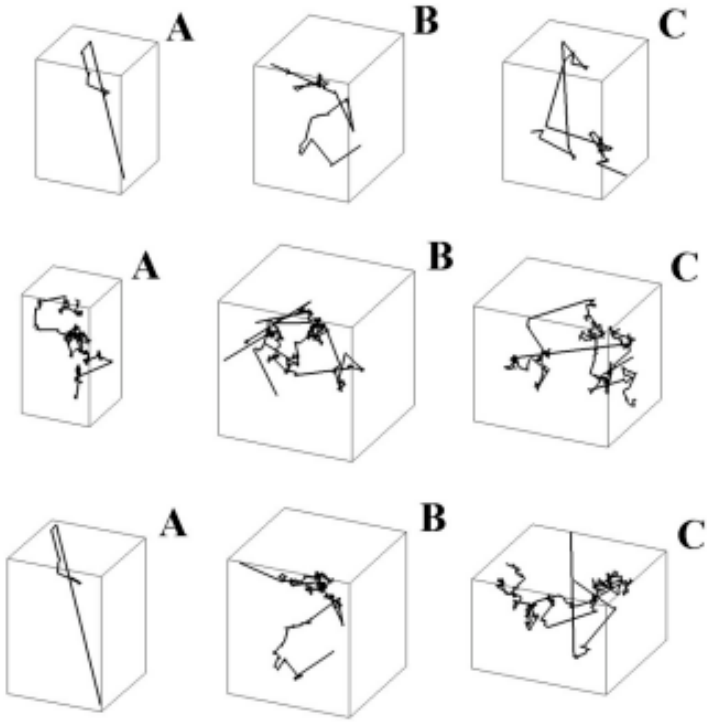

SPHERICAL COORDINATES
THE DIRECTION OF THE NEXT STEP
IS ANALYTICAL

... HOWEVER, THE STEP LENGTH
IS NOT ANALYTICAL

RANDOM NUMBER GENERATORS
IN SERIAL CODE FOR SUPERDIFFUSIVE RADIATIVE TRANSPORT

NUMERICAL GENERAL TRANSFORMATION METHOD
IN MONTE CARLO TRAJECTORIES

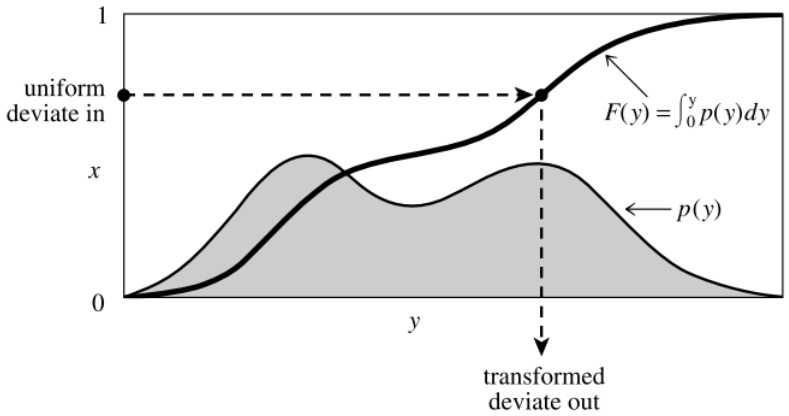

Figure 7.3.1. Transformation method for generating a random deviate y from a known probability distribution $p(y)$. The indefinite integral of $p(y)$ must be known and invertible. A uniform deviate x is chosen between 0 and 1. Its corresponding y on the definite-integral curve is the desired deviate.

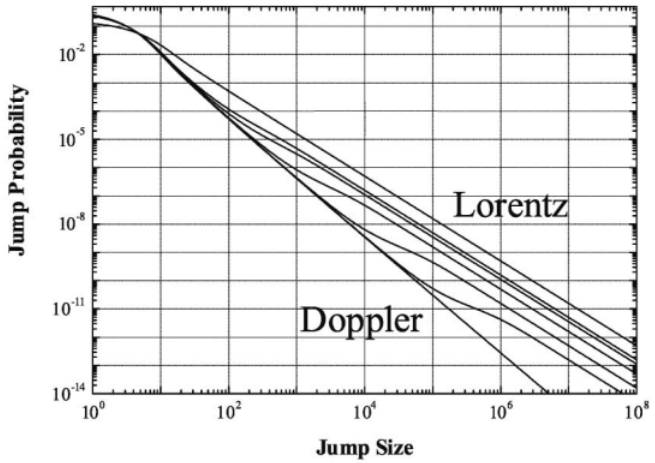

FIG. 1. Jump size distribution for CFR Doppler, Lorentz, and Voigt spectral profiles. From bottom to top: Doppler, Voigt with $a = 10^{-4}$, 10^{-3}, 0.01, 0.05, 0.1, and Lorentz.

$$p(r) = \int_{-\infty}^{+\infty} \Phi^2(x) e^{-\Phi(x)r} dx.$$

THE SINGLE STEP F(y) IS COMPUTED NUMERICALLY ONCE
IN A SET OF DISCRETE DATA POINTS

RANDOM NUMBER GENERATORS
IN SERIAL CODE FOR SUPERDIFFUSIVE RADIATIVE TRANSPORT

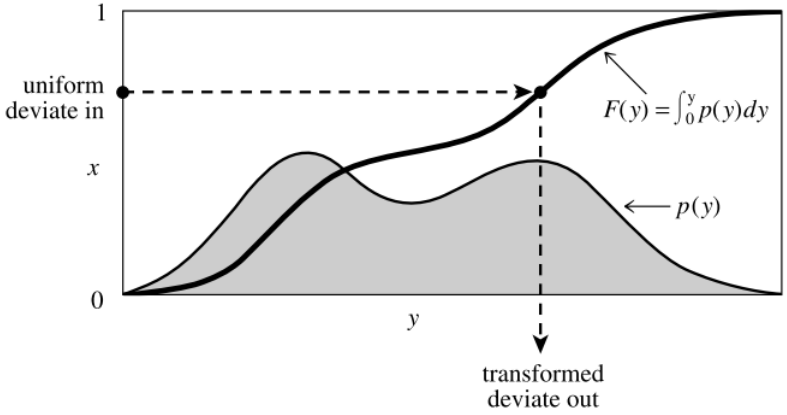

CASE I – DOPPLER

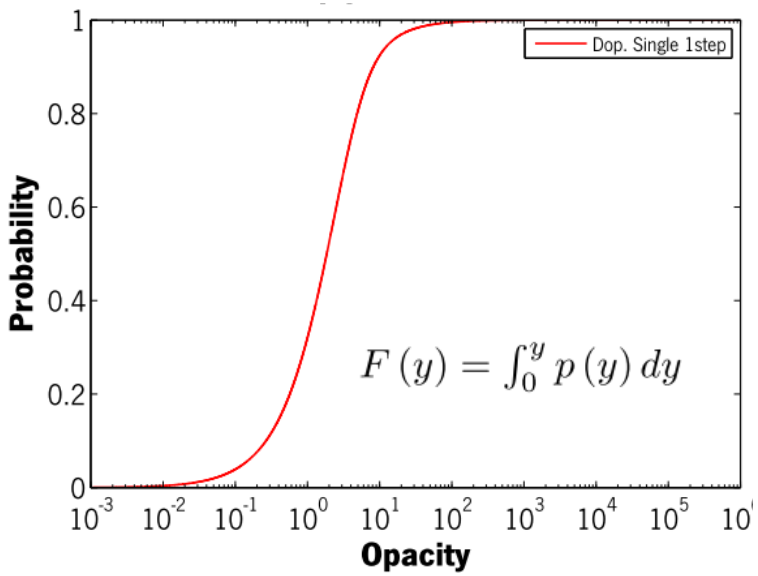

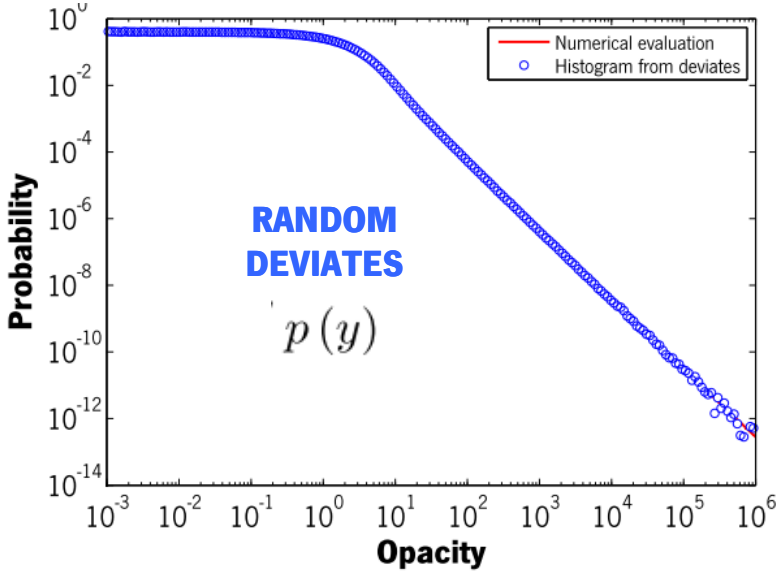

... THEN A NATURAL CUBIC SPLINE INTERPOLATION IMPLEMENTS THE TRANSFORMATION METHOD

RANDOM NUMBER GENERATORS
IN SERIAL CODE FOR SUPERDIFFUSIVE RADIATIVE TRANSPORT

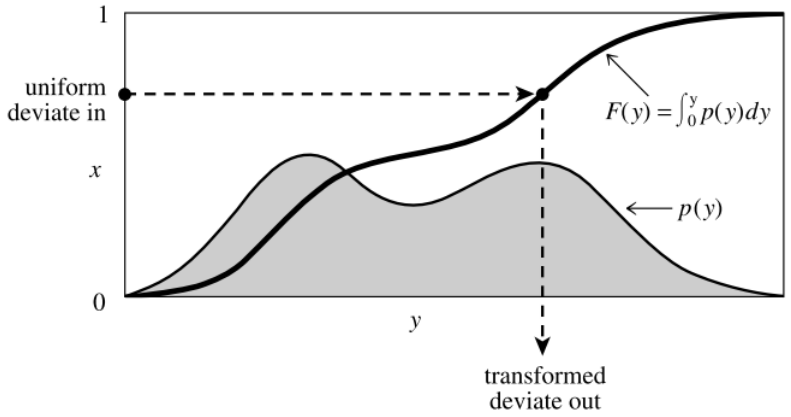

CASE II – VOIGT

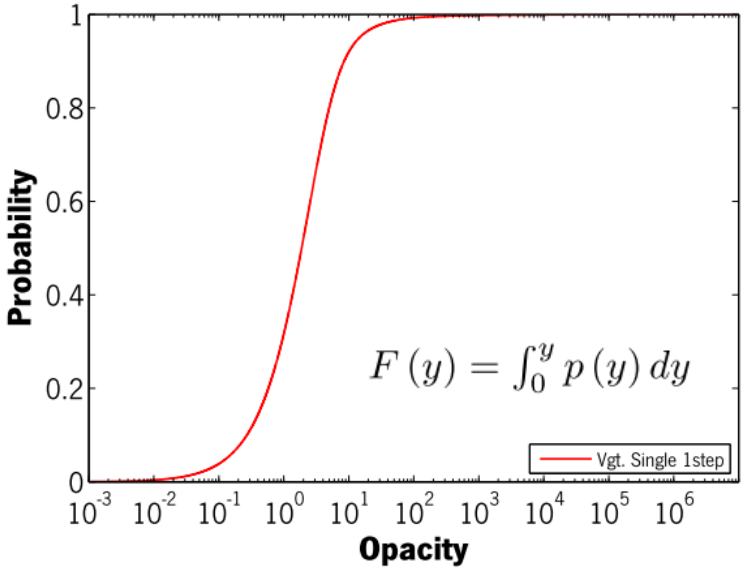

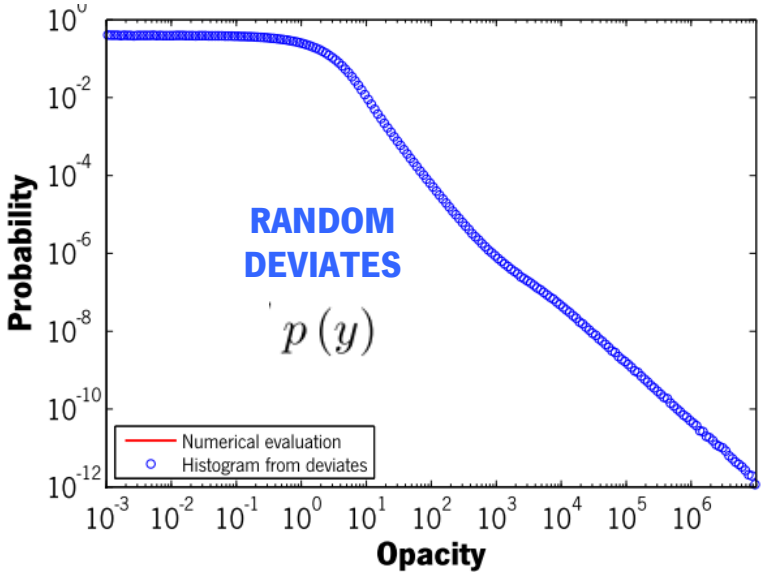

... THEN A NATURAL CUBIC SPLINE INTERPOLATION IMPLEMENTS THE TRANSFORMATION METHOD

RANDOM NUMBER GENERATORS
IN SERIAL CODE FOR SUPERDIFFUSIVE RADIATIVE TRANSPORT

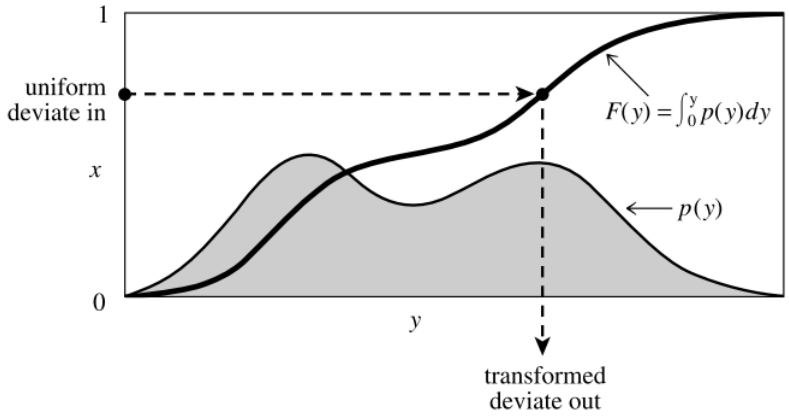

... THEN A NATURAL CUBIC SPLINE INTERPOLATION IMPLEMENTS THE TRANSFORMATION METHOD

THE CUBIC SPLINE INTERPOLATION IS A 2 STEP ALGORITHM:

- **STEP 1: SOLVE LINEAR TRIDIAGONAL SYSTEM (ONCE; NO TIME COST)**
- **STEP 2: INTERPOLATE BY TABLE LOOKUP AND BISSECTION (REPEAT ...)**

THE MONTE CARLO CODE IS EXPECTED TO SPENT MOST OF THE TIME:

- **GENERATING UNIFORM RANDOM NUMBERS IN [0,1[** $I_{j+1} = aI_j + c \pmod m$
- **IMPLEMENTING NUMERICALLY THE TRANSFORMATION METHOD (BISSECTION)**

OPPORTUNITIES FOR PARALLELIZATION (PROVIDE FEEDBACK)

MONTE CARLO PARTICLE TRANSPORT CODE FOR SUPERDIFFUSIVE RADIATIVE TRANSPORT:

- SERIAL CODE IN FORTRAN 90
- BOTTLENECK RANDOM NUMBERS (UNIFORM DEVIATES & TRANSFORMATION METHOD)
- EACH TIME A RANDOM NUMBER IS NEEDED, IS GENERATED
- FIGURE OF MERIT TO STOP SIMULATION TOTAL NUMBER TRAJECTORIES

MONTE CARLO PARTICLE TRANSPORT CODE FOR SUPERDIFFUSIVE RADIATIVE TRANSPORT ALGOTITHM:

- GENERATE TRAJECTORIES
- ACUMULATE POSITIONS
- REPEAT UNTIL TOTAL NUMBER OF TRAJECTORIES

OPPORTUNITIES FOR PARALLELIZATION (PROVIDE FEEDBACK)

OPPORTUNITY #1 – MODEL MPI

- MASTER/SLAVE MODEL WITH DYNAMIC LOAD BALANCE IN HETEROGENEOUS SYSTEMS

- TIME IS LINEAR IN # TRAJECTORIES => LAUNCH REPLICAS OF SMALL MONTE CARLO SIMULATIONS IN EACH COMPUTATIONAL NODE AND, BASED ON FEEDBACK, PARTITION TOTAL NUMBER OF TRAJECTORIES TO OBTAIN OVERALL LOAD BALANCE

- DISADVANTAGE: EACH NODE IS INDEPENDENT AND DOES NOT SHARES RANDOM NUMBER SEQUENCES

- TESTED IN PROTOTYPE CODE

OPPORTUNITIES FOR PARALLELIZATION (PROVIDE FEEDBACK)

OPPORTUNITY #2 – PARALLEL RANDOM NUMBER GENERATORS

- DATA SHARING – THE UNIFORM RANDOM NUMBER SEQUENCE IS GLOBALLY ACCESSIBLE FROM ALL COMPUTING NODES

- POSSIBLY COMBINE WITH OPPORTUNITY #1; MASTER/SLAVE MODEL WITH DYNAMIC LOAD BALANCE IN HETEROGENEOUS SYSTEMS

- NO EXPERIENCE WITH PARALLEL RANDOM NUMBER GENERATORS

OPPORTUNITIES FOR PARALLELIZATION (PROVIDE FEEDBACK)

OPPORTUNITY #3 – HYBRID CPU/GPU MODELS

- LEVEL #1: LINEAR CONGRUENTIAL GENERATOR USES INTEGER ARITHMETIC (IS THIS STILL RELEVANT TO EXPLORE, BASED IN LATEST HARDWARE?)

- LEVEL #2: RANDOM NUMBER GENERATOR BY NUMERICAL INTERPOLATION IS A "LOOKUP" ALGORITHM IN AN ORDERED TABLE; COULD BE MORE EFFICIENTLY RECODED IN GPU ?

ANOMALOUS TRANSPORT
Definitions and Examples

SUPERDIFFUSION AND LÉVY FLIGHTS
Serial code and opportunities for parallelization

DYNAMICS OF SUPERDIFFUSION
Numerical algorithms

GOAL – ALGORITHM/NUMERICAL CODE
DYNAMICS OF ANOMALOUS TRANSPORT

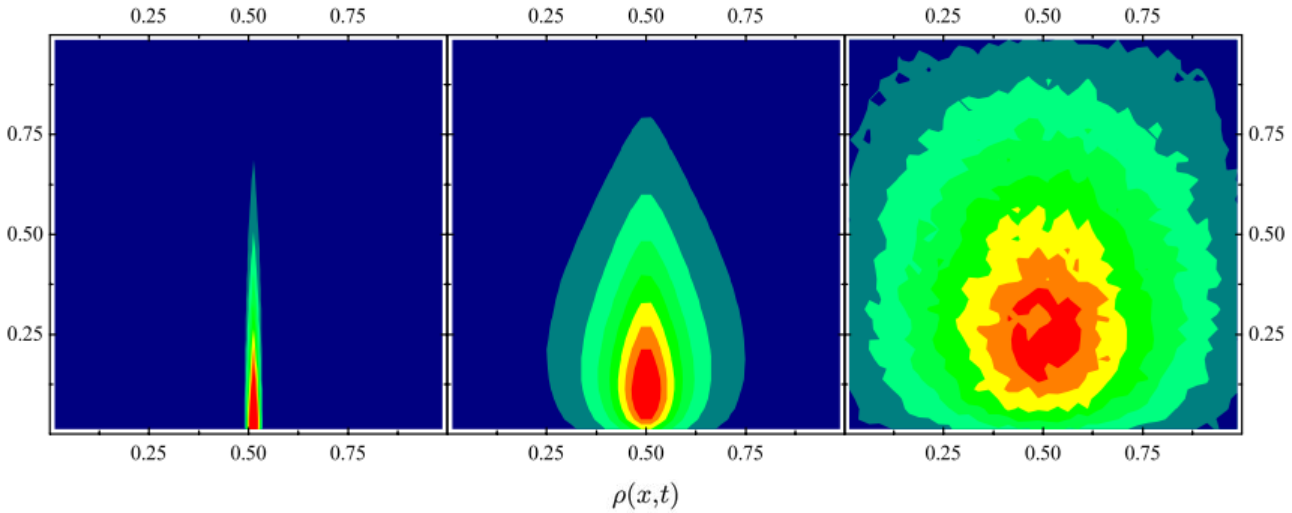

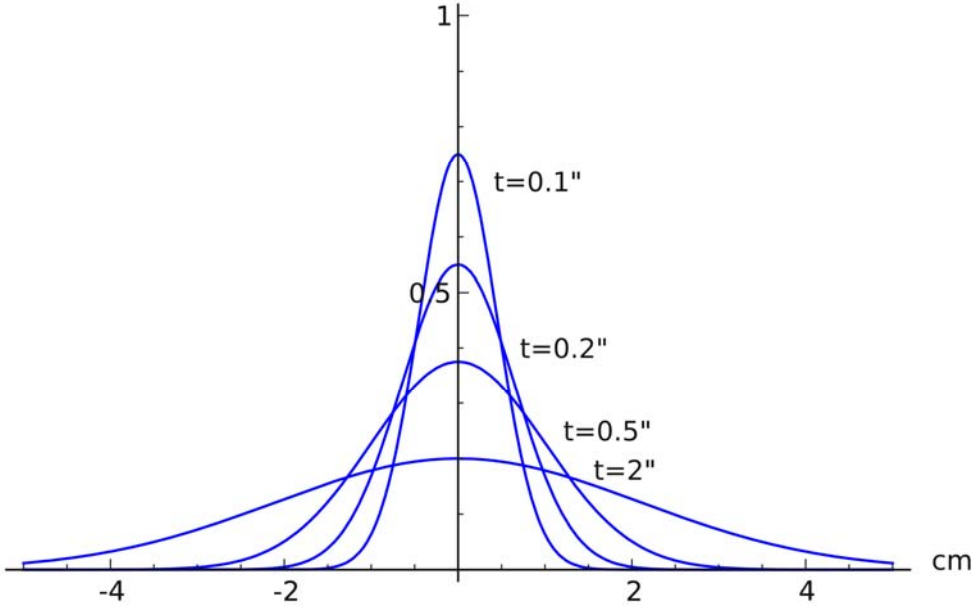

SUPERDIFFUSION (POWER LAWS)

Photon Trajectories in Incoherent Atomic Radiation Trapping as Lévy Flights

Eduardo Pereira*
Universidade do Minho, Escola de Ciências, Departamento de Física, 4710-057 Braga, Portugal

José M. G. Martinho and Mário N. Berberan-Santos
Centro de Química-Física Molecular, Instituto Superior Técnico, 1049-001 Lisboa, Portugal
(Received 19 November 2003; published 13 September 2004)

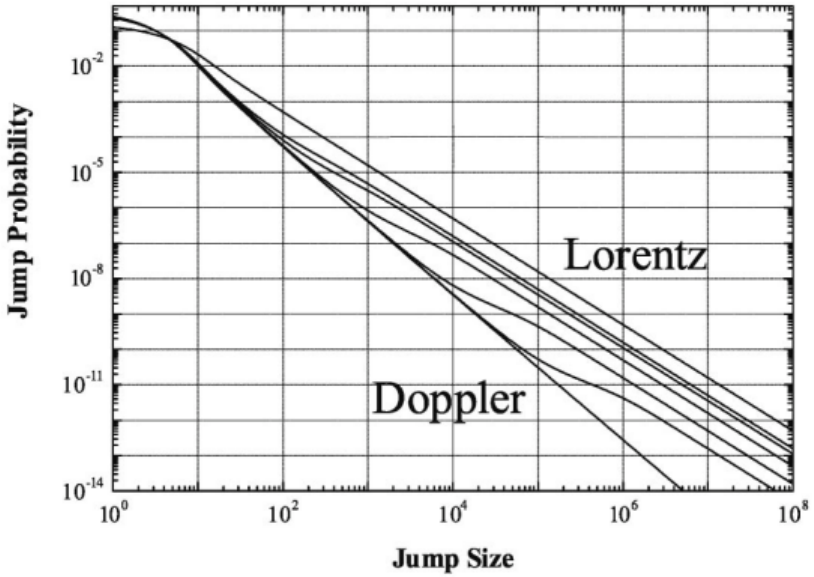

FIG. 1. Jump size distribution for CFR Doppler, Lorentz, and Voigt spectral profiles. From bottom to top: Doppler, Voigt with $a = 10^{-4}$, 10^{-3}, 0.01, 0.05, 0.1, and Lorentz.

... APPLICABLE FOR OTHER POWER LAW CASES

MASTER EQUATION

INTEGRO-DIFFERENTIAL EQUATION DESCRIBES DYNAMICS

$$\frac{\partial n(\boldsymbol{r},t)}{\partial t} = -\Gamma n(\boldsymbol{r},t) + \Gamma\phi_0 \int_V f(\boldsymbol{r},\boldsymbol{r}')n(\boldsymbol{r}',t)\,\mathrm{d}\boldsymbol{r}'$$

1. LINEAR REGIME AND EXPANSION IN "# OF JUMPS" (MONTE CARLO CODE)

$$n(\boldsymbol{r},t) = \sum_n a_n p_n(\boldsymbol{r}) g_n(t)$$

2. LINEAR REGIME AND EXPANSION IN EIGENVALUES/EIGENVECTORS

$$n(\boldsymbol{r},t) = \sum_n n_n(\boldsymbol{r})\,\mathrm{e}^{-\beta_n t}$$

3. LINEAR/NON LINEAR REGIME AND INTEGRATION MASTER EQUATION IN TIME AND SPACE

NUMERICAL ALGORITHMS

1. LINEAR EXPANSION IN "# OF JUMPS" + MONTE CARLO SIMULATION

$$n(r,t) = \sum_n a_n p_n(r) g_n(t)$$

SPATIAL DISTRIBUTIONS IN # JUMPS (MONTE CARLO)

TEMPORAL DISTRIBUTIONS ARE ANALYTICAL (DECOUPLED FROM SPACE)

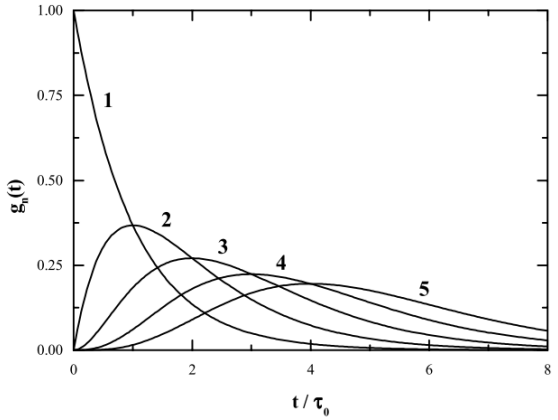

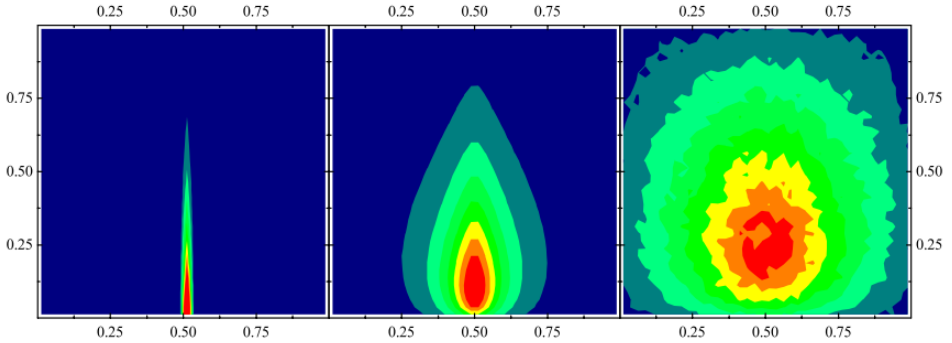

MONTE CARLO SIMULATION OF TRAJECTORIES (ONLY SPACE)
BOTTLENECK RANDOM NUMBER GENERATION/MANIPULATION

2. LINEAR REGIME AND EIGENVALUE/EIGENVECTOR DECOMPOSITION + MONTE CARLO SIMULATION (FOR RANDOM CONFIGURATIONS)

$$n(\boldsymbol{r}, t) = \sum_n n_n(\boldsymbol{r})\, \mathrm{e}^{-\beta_n t}$$

TRANSITION MATRIX FOR EACH CONFIGURATION (EIGENVALUES/EIGENVECTORS) + CONFIGURATIONAL ENSEMBLES (MONTE CARLO REPLICAS OF DIFFERENT CONFIGURATIONS)

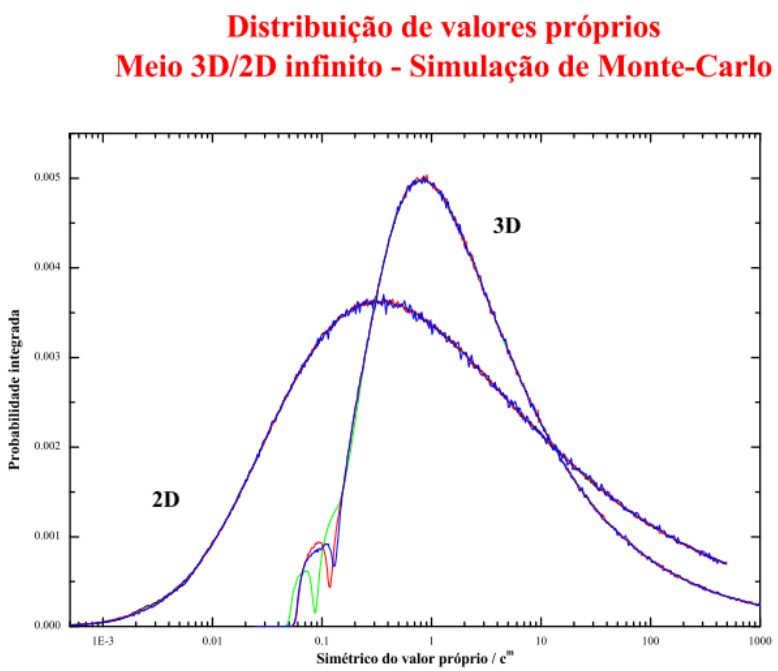

"CORE" COMPUTACIONAL LINEAR ALGEBRA (EIGENVALUES/EIGENVECTORS) + RANDOM NUMBERS
CPU or CPU/GPU HYBRID LIBRARIES

3. LINEAR/NON LINEAR REGIME USING FRACTIONAL DERIVATIVES MODELS FOR SPACE AND TIME DISCRETIZATION

$$\frac{\partial n(\boldsymbol{r},t)}{\partial t} = -\Gamma n(\boldsymbol{r},t) + \Gamma\phi_0 \int_V f(\boldsymbol{r},\boldsymbol{r}')n(\boldsymbol{r}',t)\,\mathrm{d}\boldsymbol{r}'$$

THE MASTER EQUATION CAN BE WRITTE AS A GENERALIZATION OF THE DIFFUSION EQUATION, BUT NOW USING (FRACTIONAL) DERIVATIVE ORDER

FRACTIONAL CALCULUS / FRACTIONAL DIFFUSION / FRACTIONAL KINETICS

Journal of Computational Physics 228 (2009) 3137–3153

Contents lists available at ScienceDirect

Journal of Computational Physics

journal homepage: www.elsevier.com/locate/jcp

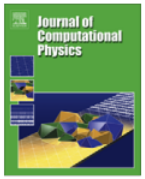

Matrix approach to discrete fractional calculus II: Partial fractional differential equations

Igor Podlubny [a,*], Aleksei Chechkin [b], Tomas Skovranek [a], YangQuan Chen [c], Blas M. Vinagre Jara [d]

3. LINEAR/NON LINEAR REGIME USING FRACTIONAL DERIVATIVES MODELS FOR SPACE AND TIME DISCRETIZATION

$$\frac{\partial u}{\partial t} = \chi \frac{\partial^2 u}{\partial x^2} \quad (t > 0,\ a < x < b)$$

@ TIME (SUBDIFFUSION)

$$ {}_0^C D_t^\alpha u = \chi \frac{\partial^2 u}{\partial x^2} \quad (t > 0,\ a < x < b)$$

fractional derivative of order α less than 1

${}_0^C D_t^\alpha$ is the Caputo fractional derivative

@ SPACE (SUPERDIFFUSION)

$$\frac{\partial u}{\partial t} = \chi \frac{\partial^\beta u}{\partial |x|^\beta} \quad (t > 0,\ a < x < b)$$

fractional derivative of the order β between 1 and 2 symmetric Riesz

"CORE" COMPUTATIONAL LINEAR ALGEBRA
"HOT TOPIC" AND matlab CODE

3. LINEAR/NON LINEAR REGIME USING FRACTIONAL DERIVATIVES MODELS FOR SPACE AND TIME DISCRETIZATION

Journal of Computational Physics 228 (2009) 3137–3153

Contents lists available at ScienceDirect

Journal of Computational Physics

journal homepage: www.elsevier.com/locate/jcp

Matrix approach to discrete fractional calculus II: Partial fractional differential equations

Igor Podlubny [a,*], Aleksei Chechkin [b], Tomas Skovranek [a], YangQuan Chen [c], Blas M. Vinagre Jara [d]

The realm of fractional kinetics is growing, and therefore it is desirable to have at hand a method for numerical solution which would be relatively simple and at the same time general enough to deal effectively with different forms of fractional kinetic equations. However, while different numerical tools for ordinary fractional equations exist and a basic framework of their numerical solution is already established, relatively few numerical methods exist to solve fractional equations with partial derivatives, and the development of effective numerical schemes is now on the agenda.

In the present paper, we propose a general approach to the numerical solution of partial fractional differential equations, which is based on the matrix form representation of discretized fractional operators introduced in [51]. This approach unifies the numerical differentiation of arbitrary (including integer) order and the n-fold integration, using the so-called triangular matrices. Applied to numerical solution of differential equations, it also unifies the solution of integer- and fractional-order partial differential equations. The suggested approach leads to significant simplification of the numerical solution of partial differential equations, and it is general enough to deal with different types of partial fractional differential equations, even with delays.